NOTICE

The quality of this microform is heavily dependent upon the quality of the original thesis submitted for microfilming. Every effort has been made to ensure the highest quality of reproduction possible.

If pages are missing, contact the university which granted the degree.

Some pages may have indistinct print especially if the original pages were typed with a poor typewriter ribbon or if the university sent us an inferior photocopy.

Previously copyrighted materials (journal articles, published tests, etc.) are not filmed.

Reproduction in full or in part of this microform is governed by the Canadian Copyright Act, R.S.C. 1970, c. C-30.

AVIS

La qualité de cette microforme dépend grandement de la qualité de la thèse soumise au microfilmage. Nous avons tout fait pour assurer une qualité supérieure de reproduction.

S'il manque des pages, veuillez communiquer avec l'université qui a conféré le grade.

La qualité d'impression de certaines pages peut laisser à désirer, surtout si les pages originales ont été dactylographiées à l'aide d'un ruban usé ou si l'université nous a fait parvenir une photocopie de qualité inférieure.

Les documents qui font déjà l'objet d'un droit d'auteur (articles de revue, tests publiés, etc.) ne sont pas microfilmés.

La reproduction, même partielle, de cette microforme est soumise à la Loi canadienne sur le droit d'auteur, SRC 1970, c. C-30.

Canada

EXPERIMENTAL CHARACTERISATION OF THE DIELECTRIC PROPERTIES OF TUMOR TISSUES

By

ARVIND SWARUP

A Thesis
Presented to the University of Ottawa
as partial fulfillment of the
Requirements for the Degree of
Master of Applied Science
In
The Department of Electrical Engineering
Faculty of Science and Engineering

ISBN 0-315-40744-1

UNIVERSITÉ D'OTTAWA
UNIVERSITY OF OTTAWA

The University of Ottawa requires the signatures of all persons using or photocopying this thesis. Please sign below, and give address and date.

ACKNOWLEDGEMENTS

The author wishes to express his most sincere gratitude to his supervisor, Dr. S.S. Stuchly, for his encouragement and guidance throughout this work. The author would particularly like to thank Dr. M.A. Stuchly, Dr. A.Kraszewski and Dr. A. Surowiec for the stimulating discussions and helpful advice during the course of this work.

Thanks are also due to Dr.S.Khadim for providing the tumor samples and for invaluable discussions on the biological aspect of the project.

Thanks are due to all the staff and colleagues of the Department of Electrical Engineering at the University of Ottawa with whom the author had the pleasure of knowing.

ABSTRACT

The in-vitro bulk electrical properties of MCA1 Fibrosarcoma induced in C57BL/6 male mice were measured at frequencies between 10 kHz and 2 GHz. Two measurement systems; an HP 3577A automatic network analyzer and an HP 8410B computer - controlled automatic network analyzer were employed. The end - of - the - line - capacitor sensor (at frequencies between 10 kHz and 100 MHz) and the open ended - coaxial sensor (at frequencies between 100 MHz and 2 GHz) were utilized as measurement sensors. Comparisons of the dielectric properties between three different stages of tumor development as well as between various locations within the tumor are presented. Differences in the dielectric constant and the conductivity were observed for the three stages. Differences in the dielectric properties of the normal surrounding tissues and the tumor tissues were also observed to be quite significant. An analysis of the data indicated a shift in the relaxation frequency of the dominant dispersion mechanism from 4.8 MHz for small tumors to 8.7 MHz for large tumors. This shift presumably reflects changes in the cellular structure during tumor development which include an increase in cell size, insertion of abnormal protein molecules and an increase in the electrolyte content in the cytoplasm. Moreover, the relative permittivity of the outer portion of a large tumor was about twice that of a necrotic portion while its conductivity was four times lower than that of a necrotic portion at 1 MHz.

CONTENTS

LIST OF TABLES

LIST OF FIGURES

CHAPTER I

Introduction

A macroscopic description of the dielectric properties of a material is provided by the complex dielectric permittivity

$$\epsilon^* = \epsilon' - j\epsilon'' \tag{1}$$

where ϵ' and ϵ'' represent the dielectric constant and the loss factor of a given material respectively. The dielectric constant describes the ability of a given material to store electric energy and the loss factor describes the fraction of energy dissipated in the material. The loss factor is more conveniently represented in terms of the conductivity (σ) of the material i.e.

$$\epsilon'' = \frac{\sigma}{\omega\epsilon_o} \tag{2}$$

where ϵ_o is the free space permittivity and ω is the angular frequency. The ratio of the loss factor to the dielectric constant ($\frac{\epsilon''}{\epsilon'}$) is frequently called the dissipation factor or the loss tangent. The frequency dependence of the three parameters (dielectric constant, loss factor and the loss tangent) provides valuable information on the nature of a given material. In this chapter, the present state-of-the-art in the electrical properties of tumor tissues, a review of some important applications followed by a brief summary of the prime objectives of the present work will be discussed.

1.1 Survey of The Dielectric Properties of Tumor Tissues

The electrical properties of biological tissues have been studied almost continuously ever since suitable techniques became available. Measurements of a number of animal

and human tissues using various techniques have been comprehensively described in literature [Kraszewski et al.,1982; Stoy et al.,1982; Stuchly and Stuchly, 1980; Tinga and Nelson,1973; Surowiec et al.,1986]. In this study we focus our attention on the dielectric properties of tumor tissues.

In order to extract an exploitable advantage from the electrical properties of tumor tissues it is necessary to obtain a precise knowledge of the dielectric properties of normal and tumor tissues as well as the dependence of these properties on frequency and on tumor development.

The earliest work known to be reported on tumor tissues was in 1926 by Fricke and Morse [1926]. They showed that the permittivity of human breast tumor tissue was higher than that of the normal tissue at 20 kHz and suggested the feasibility of diagnosis of the tumor based on this difference. After the development of microwave technology, transmission lines and waveguides became available for dielectric measurements in the microwave region of the electromagnetic spectrum. England and Sharples [1949],and Cook [1951] independently measured complex permittivity of tissues at microwave frequencies. Singh et al. [1979] developed an in-vivo technique, and measured the dielectric constant of various tissues including human breast normal and tumor tissues at frequencies from 0.1 Hz to 1 kHz. They compared the results of normal, benign and malignant breast tumors and found the differences to be clinically useful. Schepps and Foster [1980] showed that at microwave frequencies, 0.01 GHz to 17 GHz, the dielectric properties of various canine normal and tumor tissues correlate well with their water content. They also provided simple formulae to estimate the dielectric properties of soft tissues on the basis of the net water content. Joines et al.[1980] performed an interesting study on the differential absorption of microwave power between normal and

malignant tissue. Their study was based on an earlier work by Purdome et al. [Purdome et al., 1958]. This work points out that the transformation of normal to malignant tissue is accompanied by an increase in negative electric charge carried by the cells thereby increasing the mobile charges on the outer surface of the cellular membrane resulting in an increase of electrical conductivity of the tissue. Joines further showed that since ϵ' and ϵ'' are functions of frequency, an optimum frequency may exist at which the electromagnetic energy absorption of the malignant tissue is greater than that of the normal tissue. The data demonstrate that the malignant tissues preferentially absorb EM energy at 180 MHz and 300 MHz. This not only suggests a therapeutic advantage, but also that these frequencies may be of potential use in diagnosing tumors. Significant differences in the dielectric constant of mice tumors in a broad frequency range (50 MHz to 10 GHz) were first reported by Rogers et al [Rogers et al.,1983]. It was shown that the dielectric constant of mice tumor tissue was significantly larger than that of the normal muscle tissue at frequencies below 200 MHz. Similar differences in the conductivity values were also observed.

Studwell et al in 1983 [1983] used a non-invasive in vivo technique to demonstrate the differences in the dielectric properties between various normal and tumor tissues in animals and humans at frequencies from 3 MHz to 1 GHz. Brudette et al [1983] described an in-vivo technique to measure the dielectric properties of normal and neoplastic tumors in mice from 0.01 GHz to 2.0 GHz. They measured the complex impedance of a short monopole antenna inserted in a living tissue to determine the relative dielectric constant,the loss tangent and the conductivity of the tissue. Chaudhary et al. [1984] utilized frequency domain and time domain measurement techniques to expose the difference between normal and tumor human breast tissues at frequencies between 3 MHz and 3 GHz.

Recently Zywietz and Knoechel [1986] studied the effect of combined Co - γ and microwave radiation on the dielectric properties of rat tumors. They reported small differences in the dielectric properties of tumor and normal muscle tissues over the frequency range of 0.2 GHz to 2.4 GHz. Differences between the dielectric properties of irradiated and non-irradiated tumor were also reported to be small. Another important conclusion of this study is that there are small differences in the dielectric properties between vital parts of the tumor (the surface of the tumor and the necrotic parts in the tumor center). Smith et al [1986] measured the dielectric properties of implanted VX-2 carcinoma in rabbit liver and those of normal rabbit liver tissue in the low radiofrequency range (1 kHz to 13 MHz). They found the conductivity of the tumor tissue to be 6-7.5 times higher and its permittivity to be 2-5 times lower than that of the normal tissue. They attributed the large conductivity of the tumor tissues to higher water and electrolyte content and the presence of a substantial degree of necrosis in the tumor.

1.2 Applications of The Dielectric Properties of Tumor Tissues

Although the study of the dielectric properties of tumor tissues have numerous potential applications in the field of biophysics and biochemistry the importance, however, presently lies in developing suitable noninvasive techniques for diagnosis and treatment of tumor. Assessment of hyperthermia in cancer therapy requires the development of suitable methods for heating malignant tissues [Sterzer,F.,1981; Cheung,A.Y., 1982] in view of the fact that living tissues readily absorb electromagnetic energy. For this reason, quantification of the dielectric properties of neoplastic tissue as well as surrounding tissues is important in determining the optimum frequency that could be used to selectively heat tissues (uniformly) to a particular temperature. Since the absorbed energy

depends on the dielectric properties of the tissue, an estimate of energy deposition pattern within the tissue would be valuable in the assessment of potential health hazard to electromagnetic exposure of various normal organs during cancer therapy. It is essential for applicators to be designed so as to efficiently couple EM energy into the tissue. Many applicators have been designed, operating at 2.45 GHz and 27 MHz and are being used for hyperthermic purposes [Mendecki,J. et al.,1978,;Hand,J.W., 1982 Friedenthal,E. et al.,1981]. Now differences in the dielectric properties of normal and malignant tissues may offer a promising basis for radiowave and microwave imaging of tumors. For example, an in-vivo dielectric breast scanner developed by Sollish et.al [1981] is one such diagnostic technique. The scanner was based on an assumption that the dielectric properties of the normal and malignant human breast tissues were significantly different.

Besides direct utilization of the dielectric data, investigations on the possible biophysical mechanisms of the EM energy - tissue interaction would provide valuable information related to the structural changes that are accompanied during cell transformation.

1.3 Purpose of Investigation

Currently available information on the dielectric properties of tumor tissues are limited to frequencies above 10 MHz. Evidently, data at low radiofrequencies are scant except for the recent work by Smith et al. [1986]. Values of the dielectric parameters of the major relaxation processes are therefore not available. Dependence of the dielectric properties on tumor temporal development as well as the comparison of these properties within various parts of a tumor capsule (tumor surface and necrotic part) at radio frequencies have not been studied.

This work describes an experimental study of the dependance of the dielectric properties on tumor development. The study was performed in the frequency range from 10 kHz to 2 GHz utilizing a computer- controlled automatic network analyzer. Dielectric properties of different parts of a tumor capsule were also measured. In view of the importance of the differences in the dielectric properties of normal and malignant tissues, surrounding normal tissues, for example, connective tissue and body wall were studied.

CHAPTER II

Theories

The response of a dielectric material to an applied electric field is manifested by the polarization of that material. At low frequencies of the applied field the dielectric polarization is represented by the equation:

$$P(t) = (\epsilon_s - 1)\epsilon_o E(t) \tag{3}$$

where P(t) is the instantaneous polarization of the material, ϵ_s is the static dielectric constant of the material, ϵ_o is the dielectric constant of free space and E(t) is the instantaneous electric field. In the case of rapidly varying field, equilibrium cannot be maintained instantaneously and the polarization will be out of phase with the applied field. A complex notation is used to describe both the phase and magnitude of the polarization in relation with the applied field. Then eq(3) becomes

$$P = (\epsilon^* - 1)\epsilon_o E \tag{4}$$

where P and E are complex quantities representing the polarization and the electric field respectively. ϵ^* is written as eq(1) and is called the complex permittivity of the material. The phase lag between the polarization and the applied field leads to an absorption of energy and consequent heating of the medium. The rate of conversion of electrical energy to heat in the material is determined by the loss factor ϵ'' of the material. The loss tangent $\frac{\epsilon''}{\epsilon'}(\tan\delta)$ is often used to characterize dielectrics for electrical engineering purposes and can have values ranging from less than 10^{-4} for low loss materials to

more than 1 for very lossy materials like tissues. The loss tangent is also known as the dissipation factor and is identified as the ratio of energy lost to energy stored. A perfect dielectric does not absorb energy from the electromagnetic field and hence an electromagnetic wave can be propagated through the medium unattenuated. A lossy dielectric by definition has finite conductivity due to the motion in the form of free charges (conduction loss) and molecular rotation (dielectric loss). Both these processes result in energy transfer from the field to the medium.

2.1 Dielectric Dispersion

The dependance of the dielectric constant on frequency can be considered to be a law that involves dispersion. The plot of the dielectric constant and the loss factor versus frequency, shown in Fig.1, has some general form for all polar compounds. At lower frequencies, the dielectric constant is equal to the static dielectric constant ϵ_s. As the frequency increases ϵ' decreases and depicts what is known as the dielectric dispersion curve. A frequency range within which the dielectric constant varies is called the dispersion region. At still higher frequencies a sharp increase followed by a decrease of the dielectric constant represents a resonance type behavior. The explanation of such a behavior of all polar compounds can be found in the electric polarization phenomena which consist of three parts :

(a) Orientational Polarization

(b) Atomic Polarization

(c) Electronic Polarization

Each part corresponds to the motion of different kinds of microscopic particles

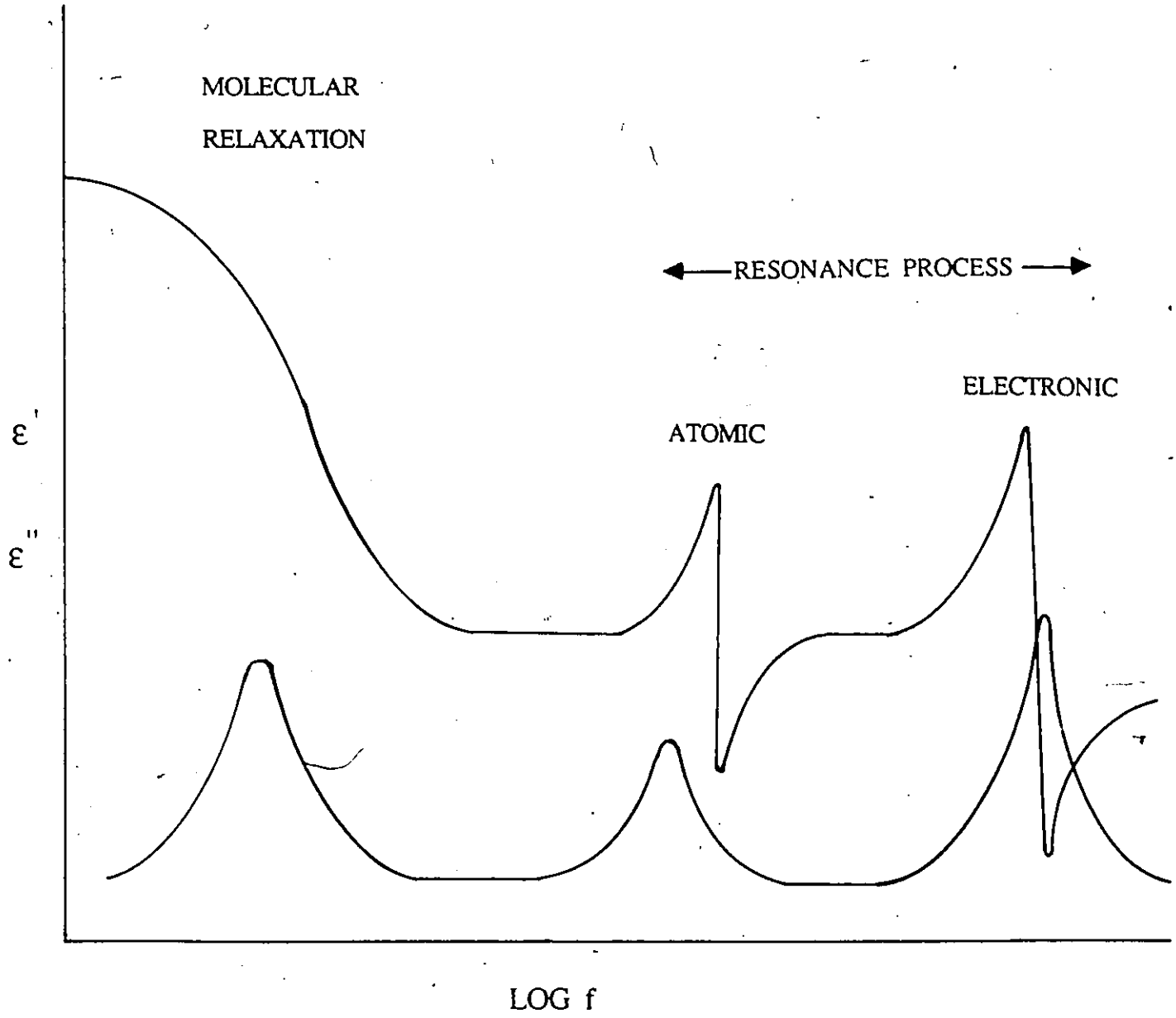

Figure 1 Dielectric dispersion curve for a polar compound demonstrating the relaxation phenomena.

(molecules and ions, atoms and electrons). The rate at which polarization can occur is limited, thus as the frequency of the applied electric field is increased some polarization will no longer be able to attain their low frequency values. As can be expected, the slowest polarization is due to dipolar reorientation and so this is usually the first polarization effect to disappear as the frequency is increased. The electrical dipoles are no longer able to align with the applied electric field and therefore the total polarizability falls. This fall, with the accompanying reduction of the permittivity, and the occurrence of energy absorption, the is referred to as dielectric relaxation. The frequency at which the decrease in orientation polarization occurs can vary from a few hertz for large macromolecules to several hundred gigahertz for small molecules. The frequencies at which the atomic and electronic dispersions occur are determined by the inertial properties of the molecules or atoms.They have a form of the resonance dispersion. The atomic polarization occurs at frequencies comparable with the natural frequency of vibration of the atoms in the molecules (10^{14} Hz). The electronic polarization occurs at still higher frequencies determined by the electronic transition between different energy levels in the atom. The difference between the dynamic behavior of orientational and induced polarization (electronic and atomic polarization) can be characterized by the dipolar orientation process which gives rise to relaxation dispersions where the frequency dependence of the dielectric loss characteristic depend mainly on the immediate environment of the molecular dipole whereas induced polarization gives rise to a number of resonance processes.

In general, the variation of the electrical properties of biological materials with frequency is due to several relaxation phenomena. Typically tissues exhibit a continuous monotonic decrease in permittivity with frequency together with an associated increase in conductivity as shown in Fig.2. Four major dispersion regions can be identified, each

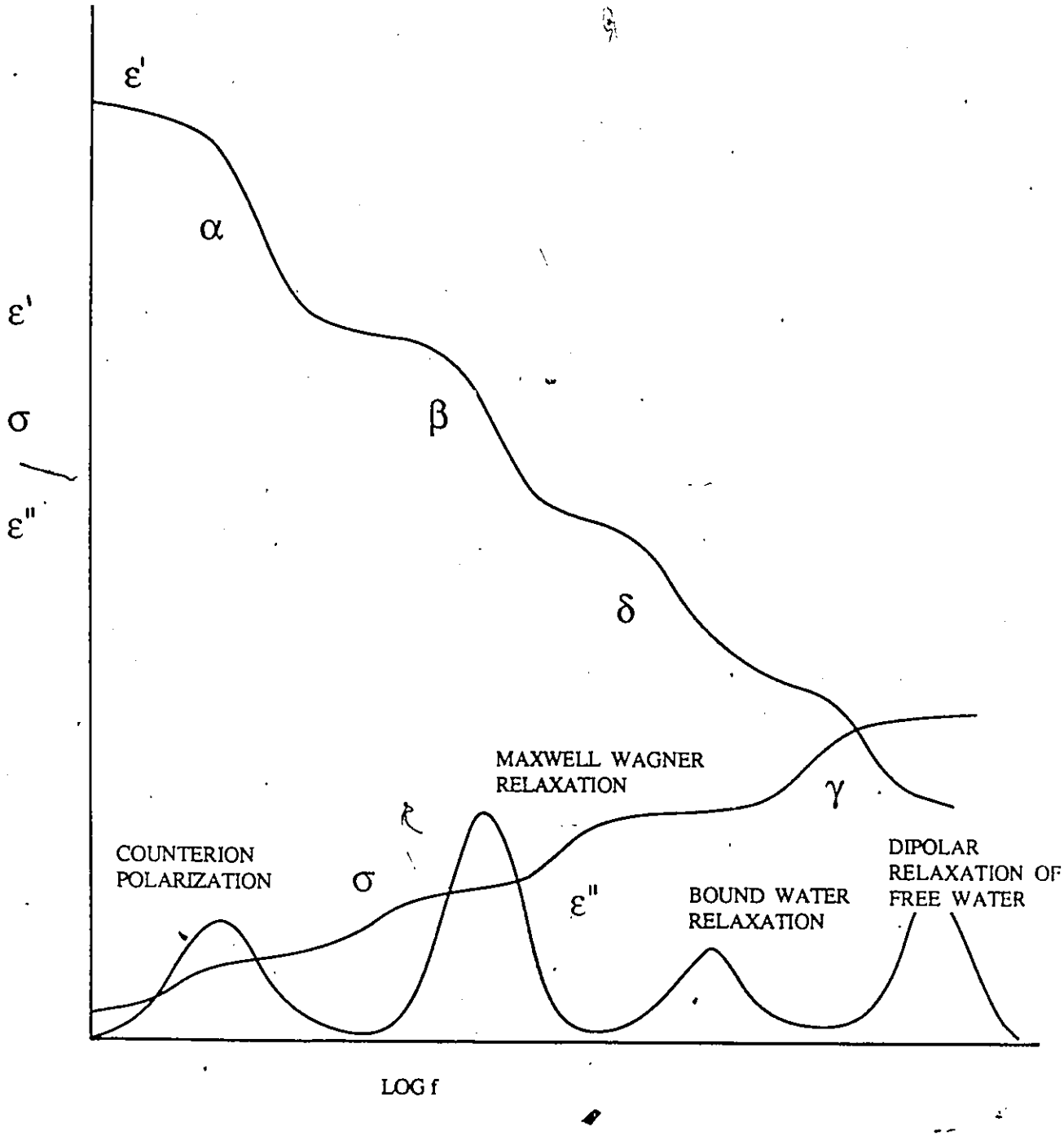

Figure 2 Variation of the dielectric constant and conductivity of a typical soft tissue as a function of frequency depicting the various dispersion regions.

characterizing a separate relaxation process. Figure 2 shows the four dispersions usually denoted as alpha (α), beta (β), gamma (γ) and delta (δ). Each of these relaxation, in its simplest form, is characterized by the equation of the type

$$\epsilon = a + \frac{b}{1 + x^2} \tag{5}$$

$$\sigma = \frac{dx^2}{1 + x^2} + c \tag{6}$$

where x is a multiple of frequency and the constants a, b, c and d are determined by the beginning and the end of the dispersion region. However, biological variability may cause the dielectric constant and the conductivity to change with frequency more smoothly than that indicated by the above equations.

2.1.1 Alpha Dispersion

The alpha dispersion is pronounced in the audio frequency range. The large permittivity values at these frequencies may be due to a number of polarization mechanisms. Some possible mechanisms that are specific to tissues would include entire membrane conduction phenomena, the charging of intracellular membranes, membrane bound organelles that connect with the outer cell membrane and the polarization of counterions on the membrane surface as proposed by Schwan (1957). Another mechanism described by Falk and Fatt (1964) explains the frequency dependence of the membrane impedance of the skeletal muscle. This mechanism arises from the rise in the tubular capacitance and resistance of the fluids between these tubules. In short the mechanism is represented by the charging of the sarcotubular system. The tissue impedance is overwhelmingly resistive at low frequencies in spite of the high permittiv-

ity values observed. A review of the present understanding and unresolved problems about alpha dispersion is provided by Schwan (1981).

2.1.2 Beta Dispersion

The beta dispersion is usually observed in the radio-frequency range. The inhomogeneous structure within the biological system is responsible for the beta dispersion, ie. polarization resulting from the charging of the cellular membrane through intra- and extra-cellular fluids. The dispersion is more commonly known as the Maxwell Wagner effect. Additional smaller contributions arise from the relaxation of protein molecules and to some extent by the relaxation of subcellular structures such as mitochondria, cell nuclei and other subcellular organelles.

2.1.3 Gamma Dispersion

The gamma dispersion is due mainly to the dipolar relaxation of water molecules. Water constitutes 80 percent of the volume of most soft tissues and has a relaxation frequency of 20 GHz at 25° C. The value of the low frequency permittivity for biosystems is less than 80. The amount by which the permittivity is lower is roughly proportional to the quantity of solute material present.

2.1.4 Delta Dispersion

Apart from the three distinct dispersions described above a fourth dispersion region between the beta and the gamma dispersion regions, has been identified. This is presumed to be due to the dipolar relaxation of protein bound water and to the rota-

tional relaxation of polar side chains and amino acids. This dispersion is characterised by several closely spaced relaxation frequencies. single dominant mechanism makes the analysis of this dispersion rather difficult.

2.2 Dielectric Relaxation Theory

The above discussion introduced the phenomenon of dielectric polarization and the associated dielectric dispersion mechanisms each characteristic of a separate relaxation mechanism. Several empirical models have been developed to mathematically relate these relaxation processes to the frequency dependence of the dielectric constant.

To illustrate a simple model the transient behavior of a biosystem is considered. Assume a step voltage applied to the material of interest placed between two parallel plates. Let the system be characterized by a single relaxation time (τ). Also assume the polarization of the system be composed of two parts, one of which arises from the orientation of molecular dipoles and the other due to electronic polarization which is considered to be instantaneous. Hence the dielectric response is an exponential function of time (t) and may be written as :

$$D(t) = \epsilon_\infty + (\epsilon_o - \epsilon_\infty)(1 - e^{(-\frac{t}{\tau})})E \tag{7}$$

where D(t) is the dielectric displacement vector, the term $\epsilon_\infty E$ arises from the electronic polarizability (i.e., the polarizability at infinite frequency or that observed at zero time after application of the electric field). The dielectric response of this system to a sinusoidal field $e^{(j\omega t)}$ may be obtained from the Laplace transformation of Eq.(1) which is given by Debye's equation

$$\epsilon^* = \epsilon_\infty + \frac{\epsilon_o - \epsilon_\infty}{1 + j\omega t} \tag{8}$$

Separating into real and imaginary parts, we get

$$\epsilon' = \epsilon_\infty + \frac{\epsilon_o - \epsilon_\infty}{1 + (\omega\tau)^2} \tag{9}$$

$$\epsilon'' = \frac{(\epsilon_o - \epsilon_\infty)\omega\tau}{1 + (\omega\tau)^2} \tag{10}$$

The above equations can also be derived in terms of the conductivity of the material from the time dependence of the current density

$$\sigma^* = \sigma_\infty + \frac{(\sigma_o - \sigma_\infty)}{1 + j\omega\tau} \tag{11}$$

Eqs.(9) and (10) are known as Debye Dispersion formulae and they refer specifically to the situation where equilibrium is attained exponentially with time when a constant electric field is imposed on the dielectric. Plotting ϵ'' against log f results in a symmetrical curve (see Fig.3) with a single maximum at $f = \frac{1}{2\pi\tau_m}$. At this frequency $\epsilon'' = max = \frac{1}{2}(\epsilon_s - \epsilon_\infty)$. This equation provides a useful check on the applicability of the Debye equations.

For small and relatively simple molecular structures there is only a single orientational process defined by a single relaxation time. This can be best represented by the Debye's dispersion formula given above. But for complicated macromolecular systems, the dielectric dispersion can consist of several components associated with a combination of cooperative and isolated movements of side chains ranging upto whole macromolecular motions. This gives rise to a spread of relaxation times and a broad dispersion. Deviations from an ideal Debye type single relaxation are bound to occur for macromolecular systems.

Botcher [1973] pointed out that the orientational polarization may be approximately characterised by a distribution of several relaxation times. Hence the complex dielectric constant characterizing the behaviour of the system in harmonic fields, assuming a logarithmic distribution, can be written as:

$$\epsilon^* = \epsilon_\infty + (\epsilon_o - \epsilon_\infty) \int_{\tau=0}^{\infty} \frac{G(\ln\tau)}{1 + j\omega\tau} d\ln\tau \tag{12}$$

where

$$\int_{\tau=0}^{\infty} G(\ln\tau) d\ln\tau = 1 \tag{13}$$

If the distribution function $G(\ln\tau)$ reduces to a delta function, Eq.(12) reduces to the Debye equation with a single relaxation time. If the dependence of ϵ^* on frequency can be written in a closed form it is always possible to obtain closed expressions for ϵ' and ϵ'' by separating the real and the imaginary parts. It is not always possible, however, to obtain a closed form expression for ϵ^* from the response or the distribution function. In the literature, much attention has been paid to the problem of obtaining information about the distribution function from experimental results. Mostly, the

experimental results are in the form of values of $\epsilon'(\omega)$ and $\epsilon''(\omega)$ at a number of discrete frequency points. A graphical method that yields important qualitative information about the distribution function is the so called Cole-Cole plot. Such a plot was suggested by R.H. Cole and K.S. Cole (1941) to assess the distribution of relaxation times by plotting the loss factor ϵ'' against the real dielectric constant ϵ'. They formulated the following expression to describe the complex permittivity

$$\epsilon^* = \epsilon_\infty + (\epsilon_o - \epsilon_\infty)\frac{1}{1+(j\omega\tau)^{1-\alpha}} \qquad (14)$$

where α is the distribution factor of relaxation times and is a measure of the broadness of the dispersion. If α is unity, the Cole- Cole plot is a semi-circle with its center lying on the real axis. The expression then reduces to the Debye equation with single relaxation time. As α increases the semicircle gets depressed with its center below the ϵ' axis and indicates a process in which the relaxation times are distributed about a mean value. Fig 3. shows a Cole-Cole plot as well as a dispersion plot representing single and distributed relaxation processes. To represent skewed Cole-Cole semicircles, Davidson and Cole [1950] suggested a generalized equation given by

$$\epsilon^* = \epsilon_\infty + (\epsilon_o - \epsilon_\infty)\frac{1}{(1+j\omega\tau)^\beta} \qquad (15)$$

where β is the distribution parameter and is a measure of its skewness. Such behaviour describes a process in which a distribution of relaxation times is skewed towards the high frequency end. We can see that Eqn.(15) reduces to the Debye type when $\beta = 1$.

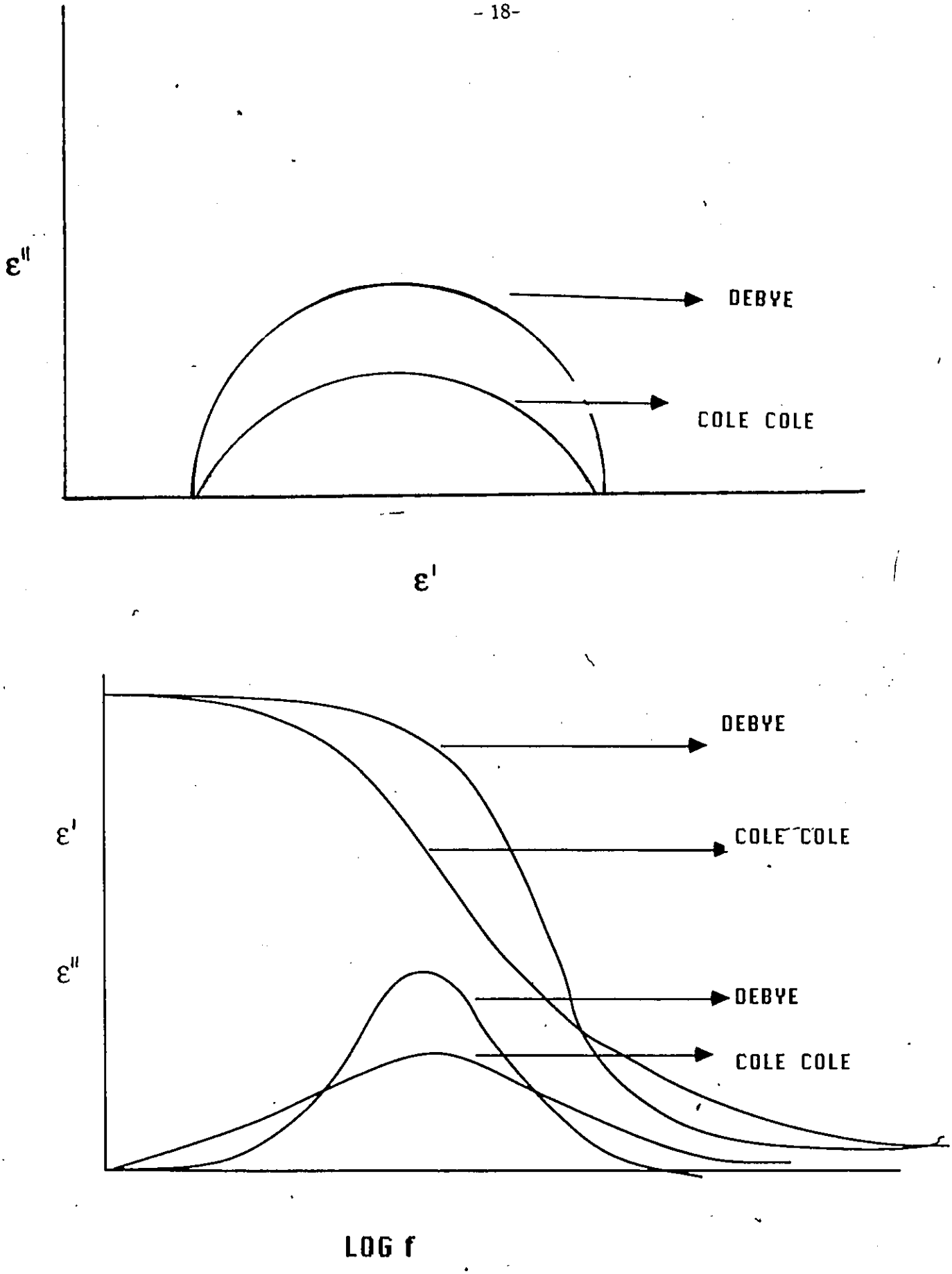

Figure 3 Cole - Cole plot showing the Debye and Cole - Cole semicircles.

For a case in which the relaxation system cannot be described by either of the above equations, Havriliak and Negami (1966) suggested a more generalized equation which encompasses both the Cole-Cole as well as the Davidson-Cole equation.

$$\epsilon^* = \epsilon_\infty + (\epsilon_o + \epsilon_\infty)\frac{1}{[1+(j\omega\tau)^{1-\alpha}]^\beta} \tag{16}$$

It can easily be seen that this equation reduces to the Cole Cole form for $\beta = 1$ and reduces to the Davidson-Cole form for $\alpha = 0$. Table I summarizes some important empirical models which have formed the basis for dielectric studies of lossy materials.

TABLE I

Summary of important empirical models

MODEL	FORMULA	CONDITIONS
DEBYE	$\varepsilon' = \varepsilon_\alpha + \dfrac{\varepsilon_0 - \varepsilon_\alpha}{1+(\omega\tau)^2}$	POLAR MOLECULES SINGLE RELAXATION TIME SEMICIRCLE (ε'' VS ε')
	$\varepsilon'' = \dfrac{(\varepsilon_0 - \varepsilon_\alpha)\,\omega\tau}{1+(\omega\tau)^2}$	
COLE-COLE	$\varepsilon' = \varepsilon_\alpha + \dfrac{(\varepsilon_0 - \varepsilon_\alpha)[1+(\omega\tau)^{1-\alpha}\sin(\alpha\pi/2)]}{1+2(\omega\tau)^{1-\alpha}\sin(\alpha\pi/2)+(\omega\tau)^{2(1-\alpha)}}$	SYMMETRICAL DISTRIBUTION OF RELAXATION TIME DEPRESSED SEMICIRCLE
	$\varepsilon'' = \dfrac{(\varepsilon_0 - \varepsilon_\alpha)(\omega\tau)^{1-\alpha}\cos(\alpha\pi/2)}{1+2(\omega\tau)^{1-\alpha}\sin(\alpha\pi/2)+(\omega\tau)^{2(1-\alpha)}}$	
COLE-DAVIDSON	$\varepsilon^* = \varepsilon_\alpha + \dfrac{\varepsilon_0 - \varepsilon_\alpha}{(1+j\omega\tau)^\alpha}$	UNSYMMETRIC DISTRIBUTION OF RELAXATION TIME SKEWED ARC

MODEL	FORMULA	CONDITIONS
HAVRILIAK-NEGAMI	$\varepsilon^* = \varepsilon_\alpha + \frac{(\varepsilon_0 - \varepsilon_\alpha)}{[1+(j\omega\tau_0)^{1-\alpha}]^\beta}$	ENCOMPASSES BOTH COLE-COLE AND COLE-DAVIDSON EQUATIONS
FUOSS-KIRKWOOD	$\varepsilon'' = \frac{\varepsilon''_m}{\cosh(aS)}$	MOLECULAR RATHER MACROSCOPIC RELAXATION TIMES

CHAPTER III

EXPERIMENTAL TECHNIQUES

In the study of relaxation processes of dielectric materials the fundamental problem reduces to the measurement of complex dielectric constant over a wide frequency range. The experimental problem involves the adaptation of existing methods to the complexities of the sample under study.

The complex permittivity of the material is generally determined by exposing the specimen to a varying electrical field (sinusoidal or transient) with frequency ranging from dc to 10^{12} Hz. This frequency range requires a number of instruments for its practical realization. Earlier techniques were designed for low frequencies (less than 100 MHz) and the measurement of the complex impedance of the specimen was accomplished using simple bridges. At frequencies above 200 MHz, measurement techniques utilize transmission lines and waveguide components and are based on controlled propagation of electromagnetic waves. At these frequencies the wave character has to be taken into account. Therefore, instead of measuring the complex impedance of the sample cell one observes the influence of the material on the properties of the wave. The amplitude and phase of the wave , reflected or transmitted through the sample are the quantities measured. Such techniques have been developed for biological materials by Von Hippel (1946), Schwan(1950), Grant (1955), and Iskander and Stuchly (1972) to name a few. A suitable experimental method depends on the frequency range to be covered as well as the permittivity values expected. Figure 4 summarizes different techniques used for the measurements of the complex permittivity in different

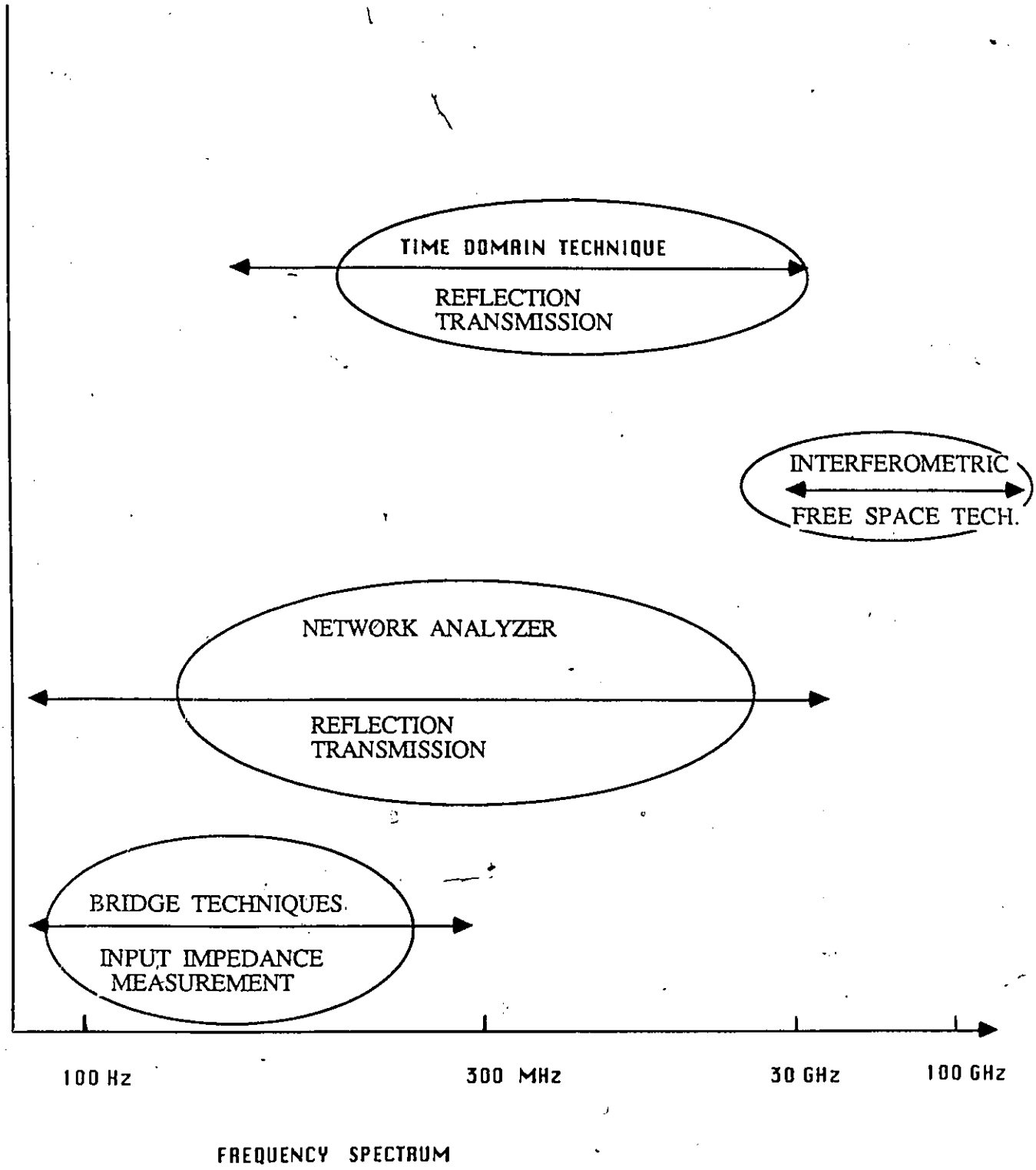

Figure 4 Summary of various dielectric measurement techniques at different frequency bands (related to biological work).

frequency ranges. As can be seen impedance bridges are used for input impedance measurements at frequencies below 100 MHz, whereas free space interferometric techniques are utilized for measurement above 30 GHz. However, a very broad frequency band is covered by broad band coaxial line technique (typically from a few Hz to about 20 GHz). In the upper frequency decade (above 10 GHz), however, use of waveguide devices make the measurement expensive and time consuming. Free space techniques, like quasi optical interferometers and open reflector arrangements are generally used for dielectric studies of low loss materials. These methods avoid conduction losses due to waveguide or resonator walls. Moreover in most open system techniques a large area of the sample is required to be exposed to the impinging waves, however, pollution of the sample during measurement is a severe problem. Low frequency measurement systems (below 100 kHz) utilized for conductive samples suffer from one major problem known as the electrode polarization. It is not possible to observe the response of the sample under test independent of the space charge polarization effect at the sample/electrode interface.

The above mentioned techniques for dielectric spectroscopy may be broadly classified into two major categories.

(a) Time domain and

(b) Frequency Domain

In this chapter a brief discussion on the Time Domain Technique will be followed by a detailed discussion of the Frequency Domain technique which is the measurement method used in the present study.

3.1 Time Domain Spectroscopy

The TDS techniques currently in use for biological work offers broad band methods for determination of one of the scattering coefficients of a specimen cell. The technique, in principle, consists of the observation of the change in the shape of a step-voltage pulse after reflection or transmission through the sample. The complex permittivity spectrum of the specimen is determined from the scattering coefficient obtained as a ratio of the Fourier transform of the response and the incident signal waveform.

An important feature of the time domain measurement is that a single record can give information over a wide range of frequencies. Another advantage is that the method usually requires only a small sample and provides a high measurement speed. Both these features are compatible with measurements of biological systems. The main disadvantage is that the upper frequency limit of the usable bandwidth of present TDS instrumentation is low. This is due to the decrease in the spectral intensity of the exciting step voltage pulses and the noise at frequencies above 10 GHz. Other important limitations are the accuracy of the measurements and availability of commercial system.

A block diagram of a TDS system is shown in Fig.5. The arrangement consists of a pulse generator (tunnel diode) which produces a fast rise pulse (of the order of a few picoseconds), a sampler which transforms a high frequency signal into a lower frequency output and an oscilloscope, or any other display or recording system. A train of fast rise step pulses from the pulse generator is applied to a transmission line, (usually coaxial) with a 50 ohm characteristic impedance. The resultant wave form (transmitted or reflected) in the line is observed at some point by a voltage probe connected to a sampling oscilloscope, or other data acquisition system.

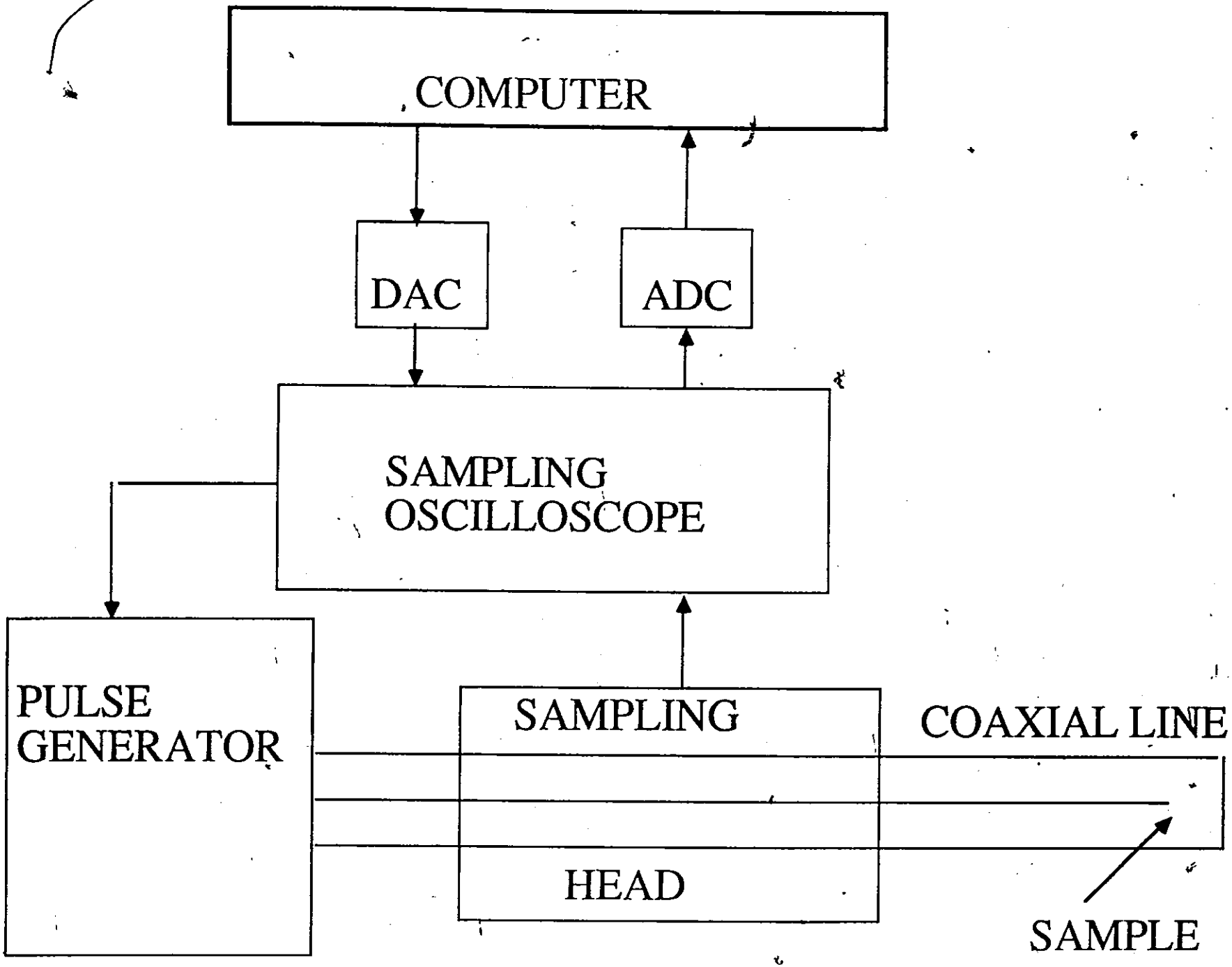

Figure 5 Block diagram of Time Domain Stectroscopy (TDS) System.

For a test specimen placed in a section of a coaxial line the reflection and transmission coefficients are given as (Cole, [1977])

$$S_{11}(\omega) = \frac{V_r(\omega)}{U_i(\omega)} = \frac{\int_{-\infty}^{\infty} v_r(t)e^{-j\omega t}\,dt}{\int_{-\infty}^{\infty} u_i(t)e^{-j\omega t}\,dt} \tag{17}$$

$$T(\omega) = \frac{V_t(\omega)}{U_i(\omega)} = \frac{\int_{-\infty}^{\infty} v_t(t)e^{-j\omega t}\,dt}{\int_{-\infty}^{\infty} u_i(t)e^{-j\omega t}\,dt} \tag{18}$$

where $U_i(\omega), V_r(\omega)$ and $V_t(\omega)$ represent the Fourier transforms of the incident, reflected and transmitted signals. The reflection and transmission coefficients in terms of the transmission line parameters are:

$$S_{11}(\omega) = \frac{Z_{in}(\omega) - Z_o}{Z_{in}(\omega) + Z_o} \tag{19}$$

$$T(\omega) = \frac{2Z_{in}(\omega)}{Z_{in}(\omega) + Z_o} \tag{20}$$

where $Z_{in}(\omega)$ is the input impedance of the line and Z_o is the characteristic impedance of the line. Substituting the measured reflection and transmission coefficients from Eqs. (17) and (18) into Eqs. (19) and (20) the input impedance of the line can be computed which would determine the complex permittivity of the specimen

$$Z_{in}(\omega) = \frac{Z_o}{\sqrt{\epsilon^*(\omega)}} \tag{21}$$

At present TDS systems cover a broad frequency range from a few Hz to 15 GHz (Voss and H.Happ 1984; Boned and Payrelasse 1982). Reviews discussing the development and methodology of the TDS system have been published [Grant et al,1978, Cole,1977, van Gemert,1973, Mishra et al.1983].

The most commonly used sample cell is merely a coaxial line (standard 7 mm diameter, APC-7 connectors) of a finite length filled with the sample of interest with suitable spacers to confine the sample. The choice of sample length is usually based on the following requirements.(a) If only the initially reflected or transmitted signal is used, the sample cell must be large enough to avoid unwanted reflections. (b) If a total reflection method is used, the sample must be long enough to produce an adequate difference signal. Some of the common coaxial sample holders are shown in Fig.6.

3.2 Frequency Domain

Before the advent of swept frequency techniques bridge techniques were most commonly used at the lower end of the frequency spectrum (less than 100 MHz). Conventional methods for complex permittivity determination were centered around measurement of the input impedance of the sample cell in frequency domain. The measurement procedure requires that the test specimen be placed in a sample hoplder and the complex permittivity measured at various discrete frequencies. However,it is not possible to have one set of equipment to cover a broad frequency range.

The most common type of bridge utilized for the determination of the dielectric properties of materials is the Wheatstone bridge. Schwan and Sittel [1953] described an accurate Wheatstone bridge which permits resistance and reactance determination at frequencies from 10 Hz to 200 kHz. The capacitance-conductance bridge developed

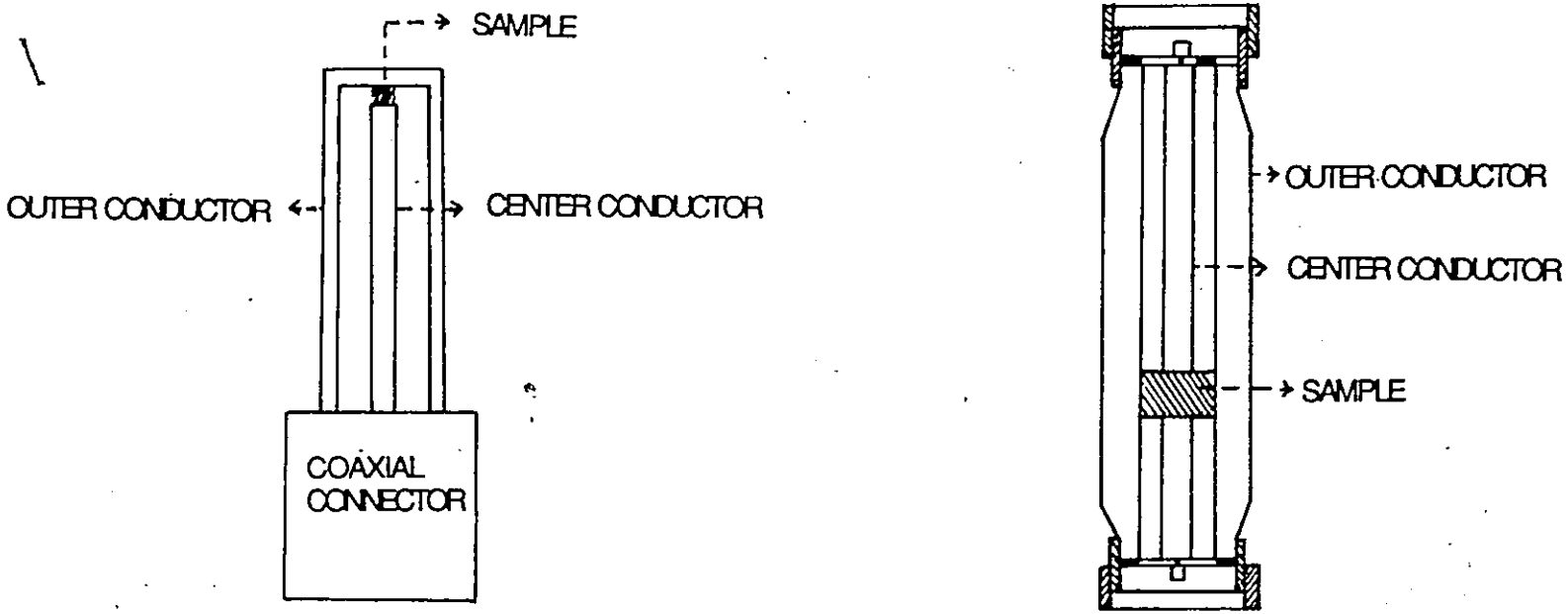

Figure 6 Some coaxial sample holders commonly used in TDS systems.

by Cole and Gross [1949] provides for fairly accurate measurements in the frequency range from 50 Hz to 5 MHz. The circuit, as shown in Fig.7, does not differ much from the Whèatstone bridge circuit except for the use of a closely coupled transformer with unity turns ratio in the equal ratio arms.

Bridge techniques are, however, not suitable for measurements above 100 MHz as the results are impaired due to errors from lead inductance. These errors become large and are strongly frequency dependent (Grant et al 1978). Another factor is that at these frequencies the wavelength is comparable to the dimensions of the sample. Hence it becomes necessary to use transmission line techniques. In these techniques the propagation constant of the electromagnetic wave in the dielectric medium is measured in order to determine the complex dielectric constant of the medium. Redheffer [1947] surveyed a number of techniques used in the determination of the dielectric properties of biological materials. Methods which used direct measurement of the attenuation coefficient and the phase constant for progressive or stationary waves in the specimen (contained in a coaxial line or a waveguide) were the most common methods. These are the Perturbation or Cavity Resonator technique and the Loaded-Line technique. The cavity resonator technique is based on measurements of a change in the resonant frequency and the Q factor of a resonant cavity by a small dielectric specimen. The real part of the dielectric constant can be deduced from the resonant frequency change and the dielectric loss can be deduced from a change of the quality factor of the cavity. However these techniques do not provide accurate results for high loss materials. Temperature control of the sample during measurement and wide frequency range are major limitations.

Loaded-line techniques in which the scattering coefficients are measured (reflection and transmission) are best suited for in-vitro measurement of biological samples.

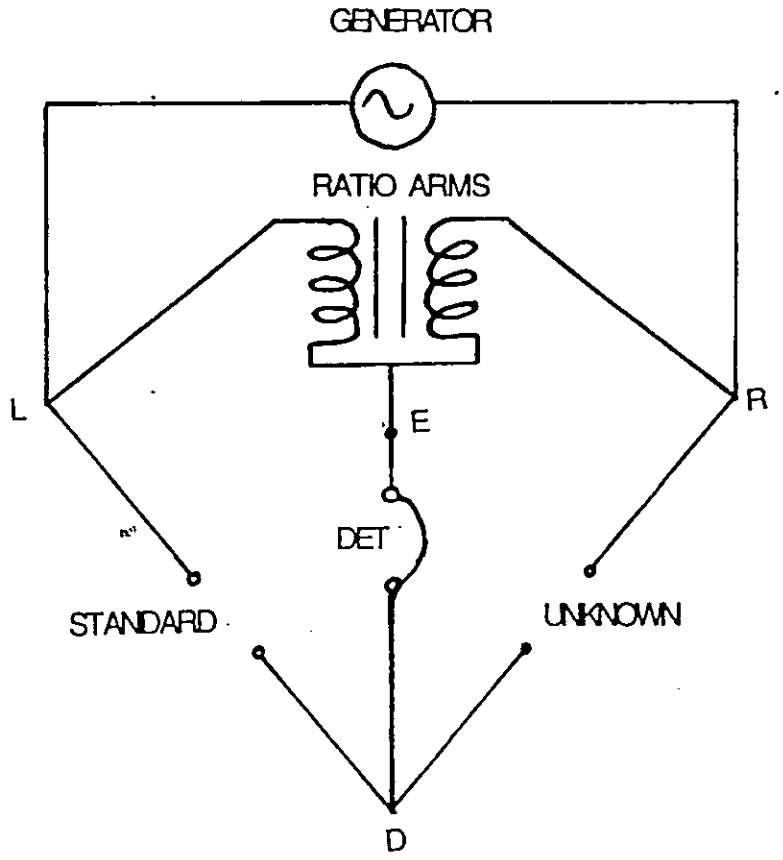

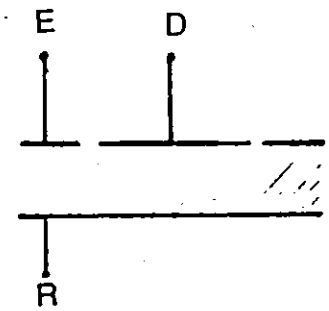

Figure 7 Circuit diagram of a three terminal bridge Technique.

In this approach the specimen fills a section of the coaxial line or a wave guide which is terminated by an arbitrary impedance. The reflection coefficient is measured at a defined reference plane (usually at the interface of the test dielectric).

3.3 Sample Holder

The choice and design of sample holders for dielectric measurements are governed by the following requirements.

(1) small sample requirement

(2) wide frequency range

(3) suitability for sample temperature control

(4) compatibility with liquid, semiliquid and solid samples

(5) size suitable to perform in vivo experiments

A parallel plate capacitor with the specimen under test forming the dielectric between the plates is frequently employed for in vitro measurements. A few of common sample holder configurations are shown in Fig.8. The accuracy of measurements is limited by two major sources of errors.

(a) Fringing Field Effects and

(b) Electrode Polarization Effects

These effects are frequency dependent and are evident in different frequency ranges. It has been shown that the observed capacitance of a parallel plate capacitor filled with a test sample is greater than the true capacitance. This is due to the effect of the fringe field at the edge of the electrode and the capacitance to ground of the high electrode.

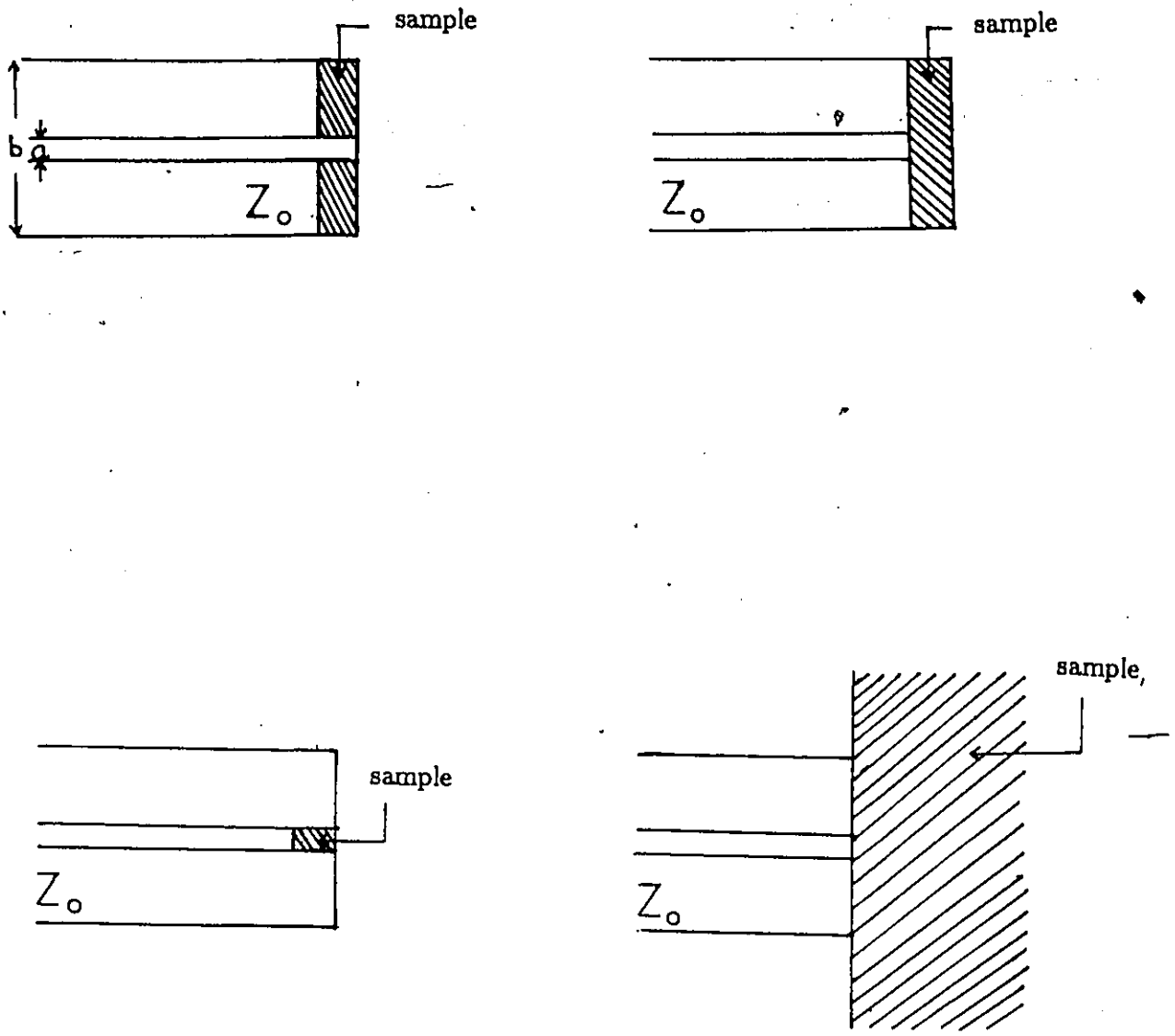

Figure 8 Sample holder configurations used in frequency domain technique

The effect of both capacitances can be eliminated by a proper cell design. For this purpose either micrometer electrode or a suitably shielded three electrode system is employed [Hartshorn and Ward,1936; Cole and Gross, 1949].

3.3.1 Electrode polarization

In order to understand the phenomenon of electrode polarization let us first discuss the reaction between metals and an ionic solution. When a metal is immersed in an ionic solution there is an imbalance between the concentration of cations and anions in the solution at the interface.The net effect is that neutrality of charge is not maintained in that region. Thus the electrolyte surrounding the metal is at a different potential than the rest of the solution. This potential is known as the half cell potential. The potential thus developed between the metal and the electrolyte is a function of the metal, temperature, frequency and is sensitive to the current passing through the electrode. Several theories have been developed to explain the distribution of ions in the electrolyte in the immediate vicinity of the metal-electrolyte interface [Ferris,1974]. These theories conclude that some sort of separation of charges exist at the metal electrolyte interface that results in an electrical double layer. Electrodes were thus described in terms of the reactions at the double layer. Electrodes in which no net transfer of charge occurs across the metal electrolyte interface were designated as perfectly polarized. It should be apparent that a truly polarized electrode has all the characteristics of a capacitor. Those electrodes in which unhindered exchange of charge is possible are perfectly nonpolarizable. When alternating current flows through such an interface a potential drop occurs. This results in equating the electrode - electrolyte interface to a series combination of resistance R and capacitance C. Thus the alternat-

ing current aspect of the electrode polarization results in in the polarization impedance which is frequency dependent. The measured alternating impedance differs from the sample impedance by the polarization impedance. The equivalent circuit representation of this impedance is shown in Fig 9. A series combination of R_p and C_p in series with the sample impedance R_s and C_s forms the total impedance observed (where R_p and C_p is the polarization resistance and capacitance respectively). Analyzing the above circuit the total resistance and the total capacitance is given below.

$$R = R_s + R_p + (R\omega C^2)R_s \tag{22}$$

$$C = C_s + \frac{1}{R^2\omega^2 {C_p}^2} \tag{23}$$

The total capacitance predominantly reflects either the true sample capacitance at high frequencies or the electrode polarization at low frequencies.The frequency dependence of C_p and R_p was first shown by Fricke [1932]. Fricke suggested that the polarization capacitance varies as f^{-m} and the polarization resistance varies as f^{m-1} where m is a constant describing the rate at which the capacitance or resistance decreases with increasing frequency .

The electrode polarization impedance can also be characterized by a phase angle, where the tangent of the angle is given by the ratio of the real to the reactive component ($\tan\theta = \omega C_p R_p$).

As indicated by Ackmann and Sietz (1984) the equivalent values for the resistive and capacitive components of an electrode-electrolyte interface also depends on the current density used to make the measurements. In order to show the dependence of

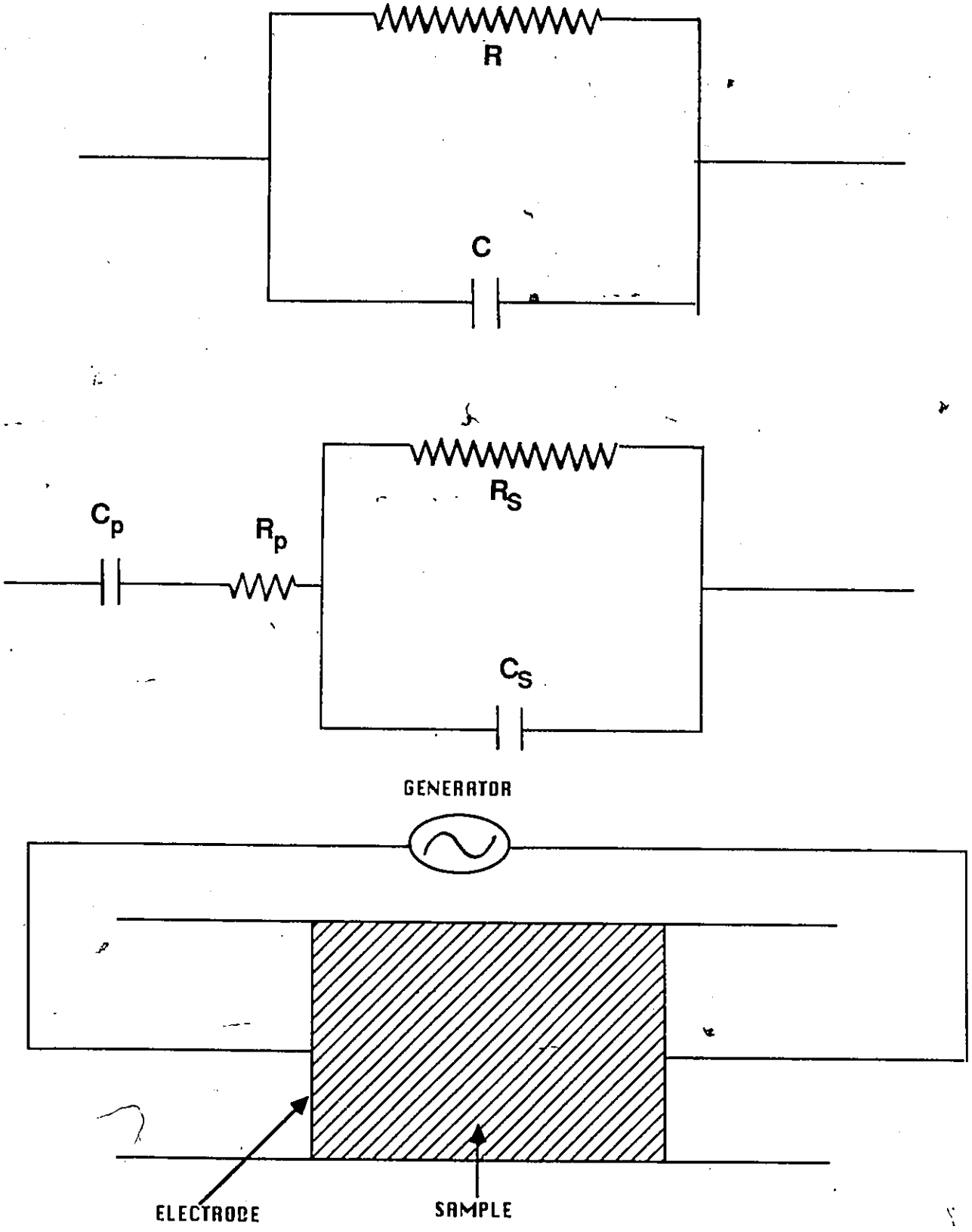

Figure.9 Equivalent circuit of a sample holder representing electrode polarization impedance.

series equivalent resistance and capacitance on the current density Geddes et al. (1971) measured these quantities using steel electrodes in contact with 0.9 saline solution. Schwan and Maczuk (1965) defined the ac 'limit current of linearity' of electrode polarization as that current for which the polarization capacitance exceeds 10 percent of its value for vanishingly small current. Simpson et al [1980] recently extended this work to investigate the effect of dc currents on linear and non-linear polarization impedances. Operating in the non-linear region results in irreversible electrochemical reactions. Furthermore Frickes equation no longer applies and therefore cannot be used to correct the measurement values. Thus in making impedance measurements care should be taken that electrodes operate in the linear region.

3.3.2 Electrode Polarization Correction

The most common method for reducing electrode polarization impedance is by depositing colloidal platinum (platinum black) on platinum electrodes. Platinum electrodes are selected as they exhibit lower polarization impedance when compared to those of other materials. They also permit the application of fine porous coat of platinum black which helps in reducing the polarization impedance by increasing the surface area of the electrode that is exposed to the electrolyte. The usual procedure for depositing platinum black on platinum electrodes was given by Kohlrausch (1897). Intensive work was later carried out by several workers to study the effect of various amount of platinum black on the polarization resistance and capacitance as a function of charge density (Schwan and Maczuk [1965] and Jones and Bolinger [1935]). This treatment increases the surface area of the electrode thus increasing the capacitance and decreasing the capacitive reactance and the resistance. A significant reduction of

electrode impedance is achieved by this method. To obtain electrodes of low polarization impedance Maczuk (1965) and James and Bollinger (1935) studied the effect of various amounts of platinum black on C_p and R_p as a function of the charge density. They found the minimum polarization impedance for a charge density of 63 C/cm^2. Schwan [1963] has given a detailed procedure for preparation of platinum black electrodes. He pointed out that his parameters apply to electrodes with a surface area greater 1mm^2. Geddes(1971) later summarized that the optimum parameters for platinizing a platinum electrode are a current density of 10mA/cm^2 and a deposition rate of about 30 to 60As/cm^2. Cole and Kishimoto (1962) utilized a hybrid platinum electrode. They started with a silver chloride electrode which was given a heavy chloride deposit of 10^3mAs/cm^2. The electrode resistance obtained was 300 Ω for a $1cm^2$ electrode. The chlorided silver chloride electrode was platinized with 1000 to 5000 mA/cm^2. The electrode was then chlorided lightly. The electrode thus approached the best properties of both the chlorided silver electrode and platinized platinum electrode. Not much work has been reported in this electrode. However, at low frequencies the electrode impedance can be many times greater than that of the sample even after depositing platinum black on the electrodes. Four methods that are employed in common practice for the correction of the electrode polarization effect are listed below (Schwan 1963).

(a) Distance variation technique

(b) Substitution technique

(c) Frequency variation technique

(d) Four electrode method

3.3.2.1 Distance Variation Technique

The distance variation technique is used with specially designed cells in which the distance between the electrodes can be varied. The measured impedance Z_m between the cell terminals is the sum of the sample impedance Z_s and the electrode polarization impedance Z_p.

$$Z_m = Z_s + Z_p \tag{24}$$

The corresponding values at the two electrode distances d_1 and d_2 are

$$Z_{m1} = Z_{s1} + Z_p \tag{25}$$

$$Z_{m2} = Z_{s2} + Z_p \tag{26}$$

If the polarization impedances are identical for the two measurements and the sample impedance is linear with respect to cell length, the above equations can be subtracted effectively yielding the value for a sample length $d_2 - d_1$.

$$Z_{m2} - Z_{m1} = Z_{s2} - Z_{s1} \tag{27}$$

which is independent of the electrode polarization impedance. This difference in measurements can then be equated to the product of the sample conductivity and the cell constant for length $d_2 - d_1$.

$$Z_{s2} - Z_{s1} = \frac{d_2 - d_1}{A} \frac{1}{\sigma + j\omega\epsilon_o\epsilon_r} \tag{28}$$

where A is the cell area, σ and ϵ_r are the conductivity and the dielectric constant of the sample, respectively.

The distance variation technique was used by Schwan and Maczuk [1965] to control stray field effects in electrolytic cells. This technique is based on a plot of the apparent dielectric constant as a function of electrode distance. Later van der Touw and M.Mandel (1971) suggested a rather complicated method using variable electrode spacing. They expressed electrode polarization as a power series in 1/d and then attempted to calculate the low order coefficients. However this method has a frequency/conductivity limit.

3.3.2.2 Substitution Technique

The substitution technique is the method in which the sample is first measured and is then replaced by a sample of known electrical properties with a similar electrolyte concentration or similar conductivity. In this case the assumption is being made that the effects of the ions on the electrodes (known solution) are the same as those of the ions of the specimen under test.This method for correcting the electrode polarization has been effectively used by a number of workers. (Takashima 1966, Surowiec et al. 1985, 1986).

3.3.2.3 Frequency Variation Technique

This technique utilizes Frickes law. Assuming that the polarization capacitance is a power function of frequency f^{-m}, then the capacitance data at low frequencies,

where the polarization term is large in comparison with the sample capacitance may be expressed as a function $f^{-(2-m)}$. The polarization data can be then extrapolated to correct for high frequency data. Not much work is known to be reported using this technique. Other graphical techniques have been proposed Oncley (1938, Oncley and Ferry (1941), Fricke and Curtis (1937) Shaw (1942) and Takashima (1963)

3.3.2.4 Four Electrode Technique

Corrections for electrode polarization impedance described above have frequency / conductivity limitations and do not eliminate the effect completely. Measuring the impedance with "zero current", in practice a very small current the polarization impedance can be nearly entirely eliminated. This is accomplished by the four electrode system (Fig.10). In this method an excitation voltage or current is applied to the sample by means of a one pair of electrodes and the second electrode pair is used to measure the potential across a segment of the sample. If the input impedance of the potential measuring circuit is infinite, no current will flow in the potential electrodes. This method effectively bypasses the electrode polarization effect. For complex impedance measurements several bridge configuration have been reported Schwan and Ferris (1968) who proposed a four electrode null technique for frequencies between 10 Hz to 1 kHz. Berberian and Cole (1969) and more recently Hayakawa et al (1975) have developed several bridges for measurement up to 30 kHz. The method suggested by Hayakawa et al. (1975) eliminates the electrode polarization as well as the frequency independent dc conductance of the specimen. However, such systems have not been used for dielectric measurements on biological tissues.

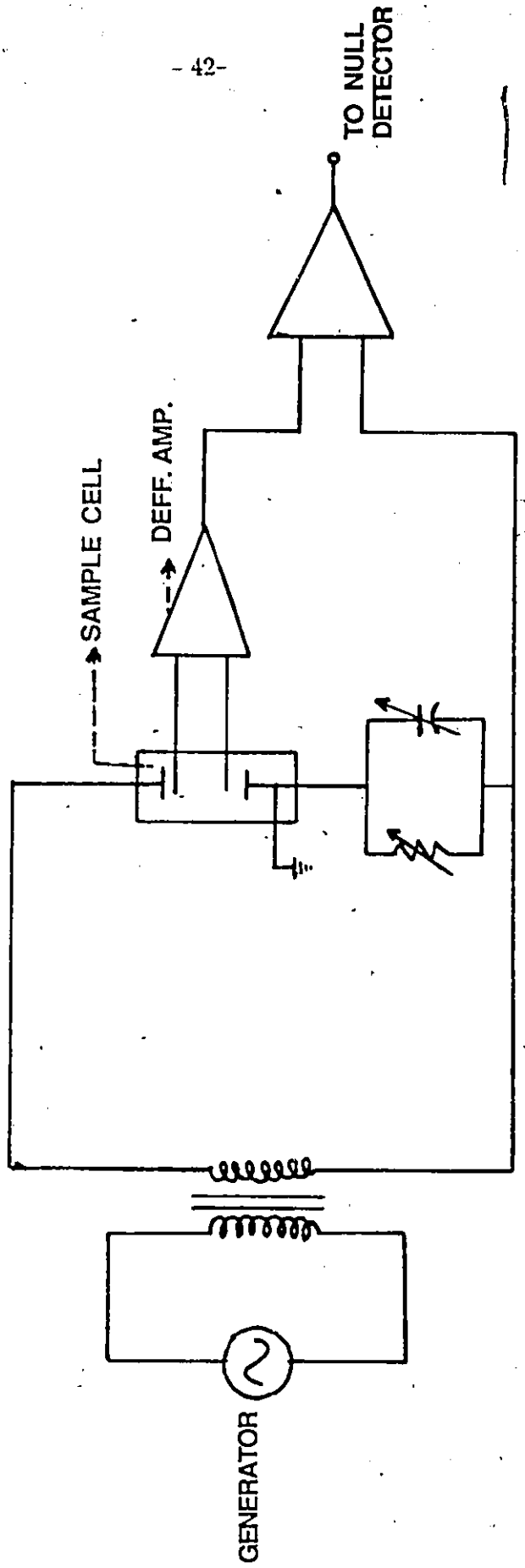

Figure 10 Four electrode sample cell cell for eleminating errors due to electrode polarization impedance.

3.3.2.5 Modern Measurement System

The most modern system in use is the computer controlled Automatic Network Analyzer. A block diagram is shown in the Fig.11. Another system the HP 3577 A used in the present study represents the state-of-the-art in instrumentation for the measurement of scattering parameters at low frequencies (5 Hz to 200 MHz). Changes in the permittivity of the sample is translated into changes in the input reflection coefficient of the sensor. The reflection coefficient is measured by comparing the magnitude and phase of the reflected waves. The sensors used for in-vivo measurements are fringe field probe systems which have been described by Stuchly et al (1982).The equivalent circuit may be represented by a parallel combination of two capacitors. The circuit consists of a lossy capacitor and a fringe field capacitance which represents the electric field concentration inside the teflon- filled part of the coaxial line. The input reflection coefficient of the coaxial line at the plane of discontinuity is given by

$$\Gamma^* = \frac{1 + j\omega Z_o[C(\epsilon^*) + C_f]}{1 + j\omega Z_o[C(\epsilon^*) + C_f]} \tag{29}$$

the complex permittivity of the sample is thus determined from

$$\epsilon^* = \frac{1 - \Gamma^*}{j\omega Z_o C_o(1 + \Gamma^*)} - \frac{C_f}{C_o} \tag{30}$$

These sensors are useful for in-vivo and in-vitro measurements of tissues from 100 MHz to 10 GHz with fairly high accuracy. Measurement at frequencies below 100 MHz a lumped capacitance method, which was developed by Stuchly et al. (1980),

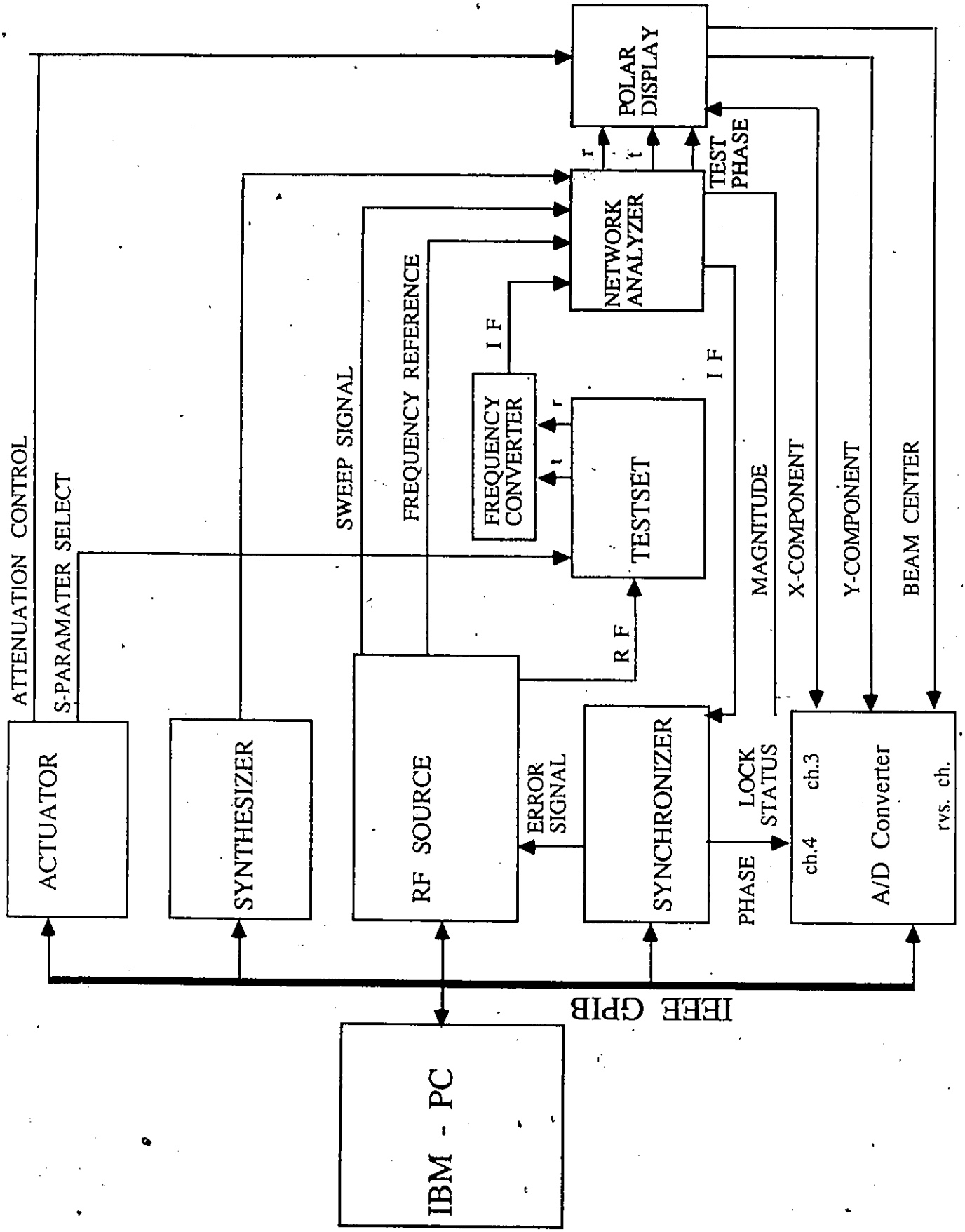

Figure 11 . Block diagram of 8410B Automatic Network Analyzer

has been used successfully by many workers (Fig.12). As shown in figure 12, a small shunt capacitor terminating the coaxial line section forms the sample holder. The total cell capacitance thus formed between the inner conductor and the short circuit is represented by the sum of the empty cell capacitance and the fringe field capacitance and is given by

$$C_T = C_o + C_f = \frac{\pi a^2}{4d}\epsilon_o + 2a\epsilon_o \ln(\frac{b-a)}{2d} \tag{31}$$

where 'a' and 'b' are the inner and the outer conductor diameters respectively and 'd' is the gap width. This expression for the total capacitance holds provided that the free space wavelength $\lambda >> (b-a)$ and $d << (b-a)$. Finally the dielectric constant and the loss factor can be obtained from the following equations

$$\epsilon' = \frac{2\Gamma_1 \sin(-\phi)}{\omega Z_o C_o(1+2\Gamma\cos\phi+\Gamma^2)} - \frac{C_f}{C_o} \tag{32}$$

$$\epsilon'' = \frac{1-\Gamma^2}{\omega Z_o C_o(1+2\Gamma\cos\phi+\Gamma^2)} \tag{33}$$

The network analyzer used for measurements above 100 MHz operates in the frequency range 100 MHz to 18 GHz.The analyser comprises of an 8410 network analyser, an HP 8745A /HP 8743A test sets an HP 8620C RF signal source, a source phase-lock subsystem consisting of an HP 8656 A synthesized signal generator an HP 8709A (option H17) synchronizer, an HP 59306A relay actuator, an HP 593134 A/D converter,

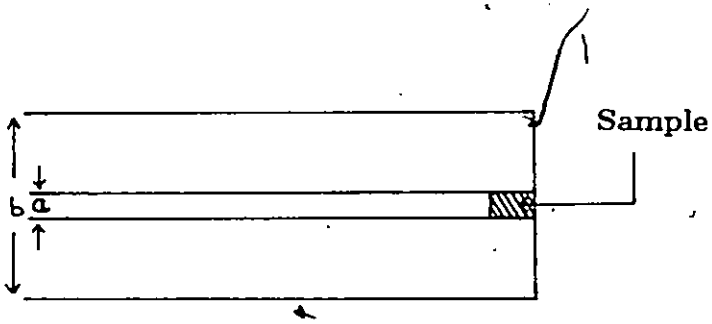

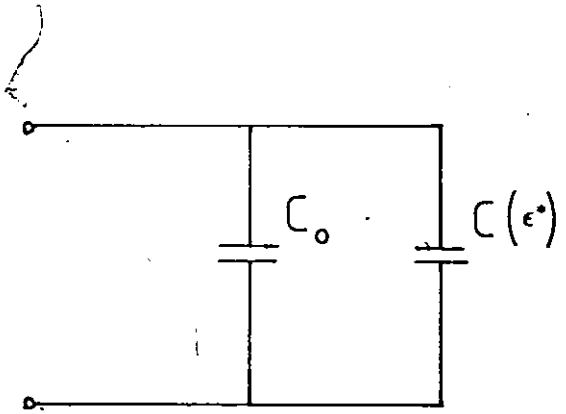

Figure 12 Equivalent circuit of the coaxial sample holder

all controlled by an IBM personal computer interfaced through an IEEE - 488 interface bus. The source phase-lock subsystem used in the measurement set up provides the synchronizer class frequency accuracy and repeatability.It improves the typical worst case open loop 8620C programmed frequency accuracy from 2.5 MHz to approximately 1 part in 10^6 plus 5 kHz, and frequency repeatability from about 300 kHz to 100 Hz. This improvement is especially valuable when measuring of properties which cause magnitude or phase of the impedance to vary rapidly with frequency. In these measurements a small frequency error can result in a significant error in the measured permittivity.

For each measurement, first the computer sets the sweep oscillator and the network analyser to the required frequency range and then routes the RF signal through the multiplexer to the test unit. The polar display IF attenuation is ranged automatically to position the trace on the display. Next, the S-parameter to be measured is selected and the resulting amplitude and phase information is digitized and transferred to the computer.

All measurement systems introduce errors into the measured results. Hence, calibration of the Automatic Network Analyser is a very important part of the measuring procedure. The measurement errors can be separated into two categories : Random errors and systematic errors. Random errors are non-repeatable measurement variations due to noise, temperature drift, and other physical changes in the test setup between calibration and measurement. These are the errors that the system itself cannot measure. These errors can only be reduced through a careful system design and by time-averaging the measurements. Systematic errors are the repeatable errors which the system can measure. They include a mismatch and leakage terms in the

test setup, isolation characteristics between the reference and the test signal paths, and the system frequency response. Since each of these errors produces a predictable effect upon the measured data, their effects can be removed to obtain a corrected value for the test device response. These uncertainties are quantified as the directivity, source match, load match, isolation, and tracking (frequency response). For the purpose of accuracy enhancement eight term or twelve term error models are utilised. For reflection measurements of one port devices the eight term error model provides a sufficient measurement accuracy. This model provides directivity, source match and frequency response vector error corrections for reflection measurements. The flow graph of the signals during the measurement of an unknown reflection coefficient is shown in Fig.13. It can be shown that the three errors are mathematically related to the actual complex value of the reflection coefficient and the measured value by the following equation:

$$S_M = E_{DF} + \frac{S_A(E_{RF})}{1 - E_{SF}S_A} \tag{34}$$

where S_A is the actual value of the reflection coefficient and E_{DF}, E_{RF}, and E_{SF} are the complex error correcting coefficients. When these coefficients are known at each test frequency, the actual value can easily be calculated from the measured value of the reflection coefficient. The error correction coefficients may be determined by calibration of the measuring system with three independent standard terminations whose reflection coefficients are known at all frequencies. The first standard applied is a 'perfect load' at the reference plane. Then $S_{11} = 0$ and the effective directivity is determined. Of course, in practice 'perfect load' cannot be achieved and any reflection from the termination

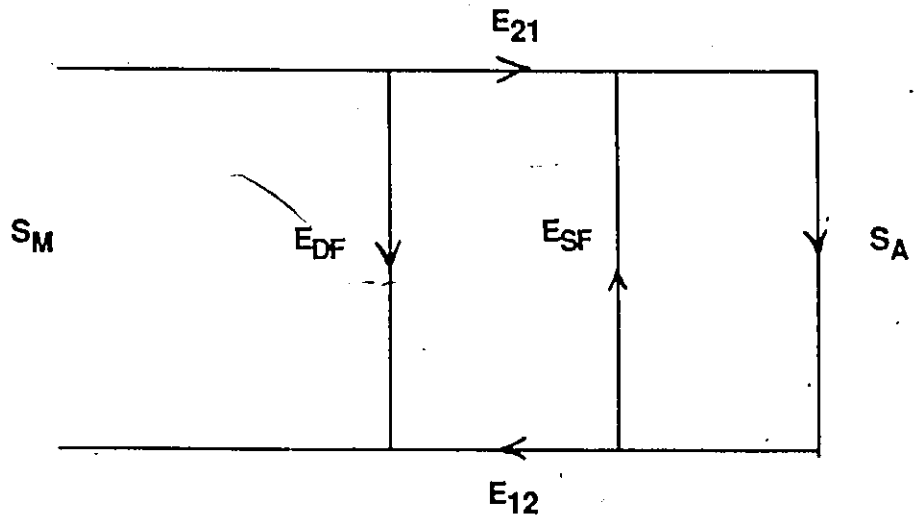

Figure 13 . Flow graph for error correction in ANA.

represents an uncompensated error. Hence the system's effective directivity becomes the actual reflection coefficient of the perfect load. In general, any termination having a return loss value greater than the uncorrected system directivity reduces reflection measurement uncertainty. Next, a short termination is used to establish one of two equations needed to determine the two unknowns E_{SF} and E_{RF}. The open circuit gives the second condition. The values of the effective source match and reflection tracking are computed and stored. Now the unknown specimen is measured to obtain the value for the measured response at each frequency. The actual value can thus be computed from:

$$S_A = \frac{S_M - E_{DF}}{E_{SF}(S_M - E_{DF}) + E_{RF}} \tag{35}$$

The application of this procedure for permittivity measurements using the open ended coaxial line creates complications which limits the accuracy. In particular a standard match load cannot be realized for open ended lines. A simple calibration technique has been developed by Kraszweski et al. (1983). In this method the probe is immersed in a liquid of well-known dielectric properties instead of a matched load. This method also requires a set of three equations to be solved to determine the error correcting coefficients. These equations are

$$S_i = E_{DF} + \frac{E_{RF}\Gamma_i}{1 - E_{SF}\Gamma_i} \tag{36}$$

for i= 1,2 and 3, where Γ_i are the known reflection coefficients, and E_{DF}, E_{RF}, E_{SF}

are the error correcting coefficients for the system directivity, frequency tracking and source match respectively. Solving the set of equations given in Eq.(36) leads to the general expression for the true value of the measured reflection coefficient during the actual measurement cycle (i=4) in the form

$$\Gamma_4 = \frac{S_4 - E_D}{E_s(S_4 - E_D) + E_R} \tag{37}$$

where S_4 is the measured value of reflection coefficient for the sensor immersed in an unknown medium. The values of the standard reflection coefficients Γ_1, Γ_2 and Γ_3 used for the system calibration are arbitrary in general, but for reason of convenience their magnitudes and phase angles should be as different as possible and invariant in time. For the present application open, short and a known liquid were used as standard terminations. The known liquid could be deionized water, methanol or saline solution of an appropriate concentration. The complex permittivities of these liquids as a function of frequency and temperature are known.

The choice of the sensor diameter depends on the frequency range in which the sample is to be tested and the optimum sensor capacitance C_o selected to obtain minimum uncertainties in the measured values of the relative permittivity and loss factor. During the measurement procedure the short circuit termination was realized by carefully pressing a metal foil to the flat surface of the sensor tip. This provided stable and repeatable short circuit. The open circuited sensor was used as the second standard termination. The input admittance of the sensor was modified to account for the fringe field capacitance in air. Thus $\Gamma_{oc} = e^{(-j2\beta l)}$ where $\beta l = \tan^{-1}(\frac{\omega G)}{Y_o}$ is an electrical elongation of the line caused by the total sensor capacitance with $\epsilon^* = 1$. For the third

standard termination the open end of the sensor was immersed in water or a saline solution. The choice of the liquid was made considering the range of the expected conductivity values of the unknown sample in the frequency range studied. It was found that a better accuracy was achieved if the conductivity of the standard liquid chosen was close to that of the test sample.

CHAPTER IV

Materials And Method

4.1 Tumors and Tumor Specimen

The specimens investigated included normal and tumor tissues. The normal tissues were the muscle (body wall) and connective tissues located close to the tumor. The tumorous tissues consisted of three stages of tumor development. These have been classified as small (7 day), medium (15 day) and large (30 day) tumors having cross-section area of approximately 60 mm^2, 430 mm^2 and 800 mm^2, respectively.

The specimen investigated included normal muscle tissue and three stages of tumor tissues grown in mice. The tumor was MCA1 Fibrosarcoma. The MCA1 Fibrosarcoma was induced in C57 BL/6 black mice at the Cancer Clinic, Civic Hospital, Ottawa. This particular line of tumor was originally derived by innoculation of 50μm of 3-Methylcholantherene (MCA) dissolved in trioctanian, subcutaneously into three week old male mice. The tumor cells were kept alive by weekly subcutaneous trocar transplant implantation into inbred mice.

The Fibrosarcoma cells initiated by the above procedure were allowed to grow in a number of animals. These animals were seperated into four categories in order to obtain tumors at different stages of development. Pathological cells were induced into the animals with a delay of one week between each animal. This resulted in four stages of tumor after one month. Out of these, three stages were selected for measurements, 7 day, 15 day and 30 day. These were classified as small medium and large tumors, respectively. The smallest tumor (7 day) had grown to a size that was found suitable for measurement purposes. The mice bearing the required tumor stage was sacrificed

(cervical dislocation) and the tumor capsule excised asceptically. Surrounding tissues consisting of connective tissues and body wall were also carefully removed. These were selected from sites that were close to the tumor. The tissues were placed in seperate plastic containers and enclosed in an ice box before transporting them to the measurement laboratory. All measurements were completed within four hours after the death of the animal. A total of 15 animals were studied (5 animal for each stage). Water content of each sample was determined using the weighing and drying procedure. The samples were weighed and heated in an oven at a constant temperature of 100 deg C. The weight of the sample was monitored every 24 hrs till constant weight was attained. The final weight of the sample was subtracted to determine the tissue total water content.

On careful examination of the cross section of the tumor capsule three distinct phases in the tumor development were observed. While a small tumor (7 day) exhibited uniformity, the medium tumor (15 day) showed the formation of necrosis at the tumor center. The large tumor (30 day) exhibited a higher degree of necrosis with the necrotic region occupying a larger volume of the tumor capsule. Two distinct regions were thus identified: the outer growing portion which is highly oxygenated, and the inner necrotic nutrient depleted region. The latter region mainly consists of dead cell fragments. The two regions were measured seperately.

4.2 Sample Preperation

After the measurement site on the tumor capsule was identified, disc shaped specimens 6.2 mm in diameter and 0.75 mm in thickness were cut out from the tumor using a conventional puncher. The disc was placed over the center conductor of sample holder. The sample holder shown in Fig.14 is essentially a modified GR-900 connector.

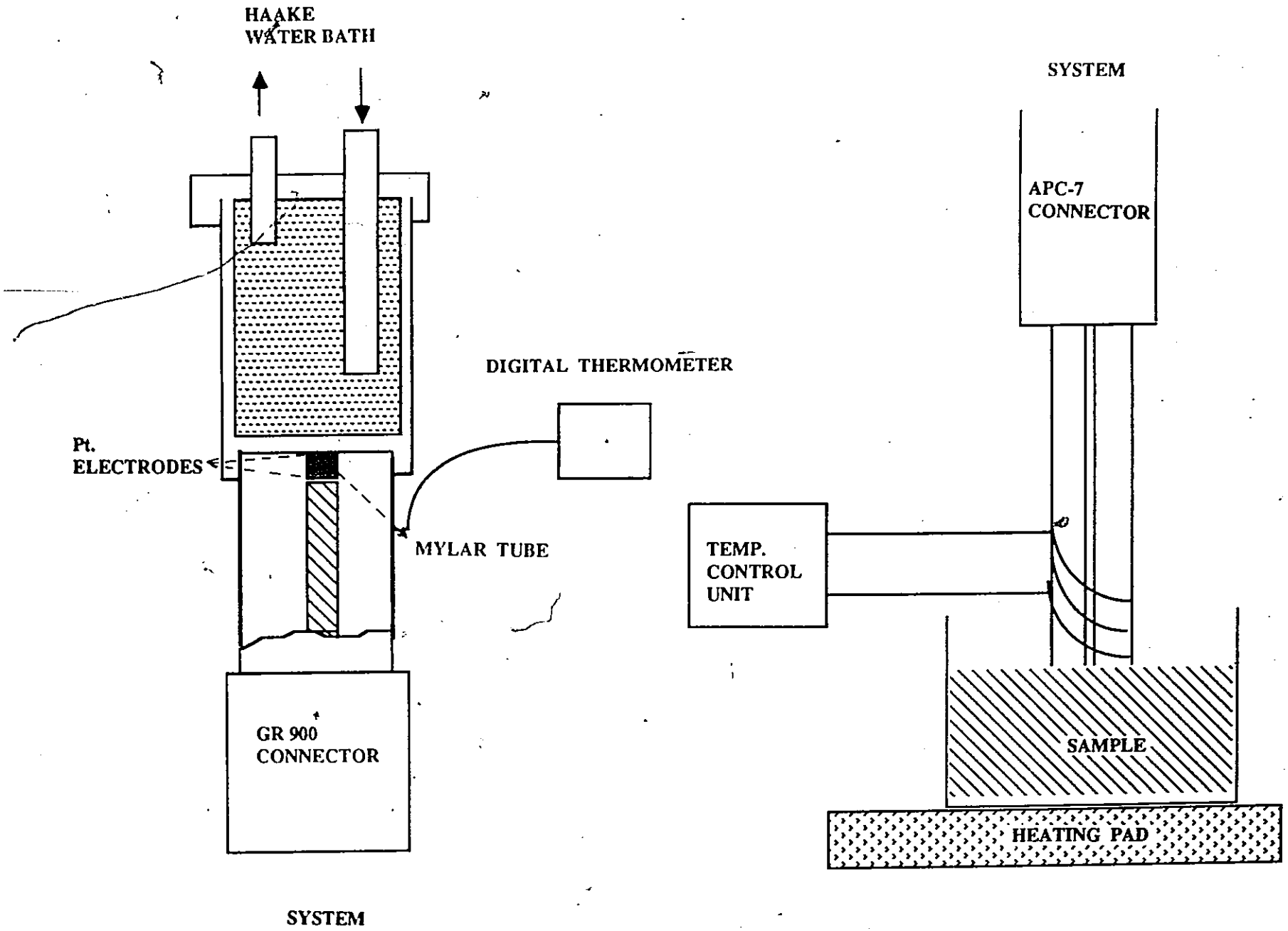

Figure 14 Experimental setup using the End-of-the-line and the open ended sensors.

The original center conductor is replaced by a cylinder of the same diameter (6.2 mm). A platinum disc covers the end of the center conductor. A thin mylar tube surrounds the center conductor as shown in Fig.15 in order to confine the sample in the required volume. The second part of the sensor consists of a shorting plate with a centrally located platinum disc and an external water jacket to control the sample temperature. Both platinum electrodes were plated with platinum black in order to minimise the effect of electrode polarization. A temperature probe was connected to the metallic connector adjecent to the sample to record the temperature of the sample using a Fluke 2176A digital thermometer. The temperature was recorded with an accuracy of 0.5° C. The temperature of the sample was maintained at $37.0 \pm 0.5°$ C. Water at constant temperature was circulated through the water jacket, connected at the top of the shorting plate, by a Haake water bath equipment. The coaxial sample holder was covered by a foam jacket to avoid loss of heat. This procedure was used for measurement at frequencies 0.01 to 200 MHz using the 3577A Automatic Network Analyser. A single scan of the above frequency range for phase and magnitude measurement of the reflection coefficient took approximately 10 s. Four hundred and one frequency points were scanned in one run making it possible to take five or six scans for each sample to provide statistically viable data. The data were stored in a floppy disc for further analysis. A computer controlled 8410B automatic network analyser was used for measurements at frequencies from 100 MHz to 2 GHz. The calibration procedure has been described in chapter III. The sensor utilized is a 3.6 mm semirigid open ended coaxial sensor. The sensor was placed in contact with the sample of a thickness greater than 3 mm. To control the temperature of the sample a heating coil was wound round the probe and connected to a temperature control unit. The temperature of the probe was maintained constant at $37 \pm 0.5°$ C. A heating pad was placed under the specimen

in order to maintain the temperature of the environment around the sample close to the sample temperature. The probe and the sample was wrapped in plastic to avoid water loss during the measurement procedure. For each sample the measurement was repeated three times at twenty one discrete frequency points.

CHAPTER V

Results and Discussion

5.1 Results

This chapter presents the results of the study carried out on mice fibrosarcoma at different stages of development performed in a broad frequency range (10 kHz to 2 GHz). A total of 15 animals were studied with five animals for each stage of tumor development. The total variability of the experimental results was 2 - 8 percent for the dielectric constant and 2 - 16 percent for the conductivity. These values include the variability among animals of the same species. The interpretations of the experimental results are later discussed.

The experimental results for the dielectric constant and conductivity of the three stages of MCA1 Fibrosarcoma are summarised in Figs. 15 and 16. The curves represent data for the outer portion of the tumor. Data from surrounding normal connective tissues and body wall (muscle) are also plotted for comparison. This demonstrates the magnitude of the differences that exists between normal and neoplastic tissues. Figures 15 and 16 also include data obtained by Rogers et al. [1983] on mice KHT fibrosarcoma at frequencies above 50 MHz and by Zywietz and Knochel [1986] on R1H Fibrosarcoma at frequencies above 200 MHz.

Figure 17 shows the variation of the loss tangent as a function of frequency and reveals a shift in the critical frequency as the tumor progresses. As the large tumor had a fairly well developed necrosis two regions within the tumor were identified and studied. Figure 18 depicts the variation of the dielectric constant and the conductivity of the necrotic region and the outer growing portion of the tumor.

MICE TUMOR (FIBROSARCOMA) DIFFERENT STAGES OF GROWTH

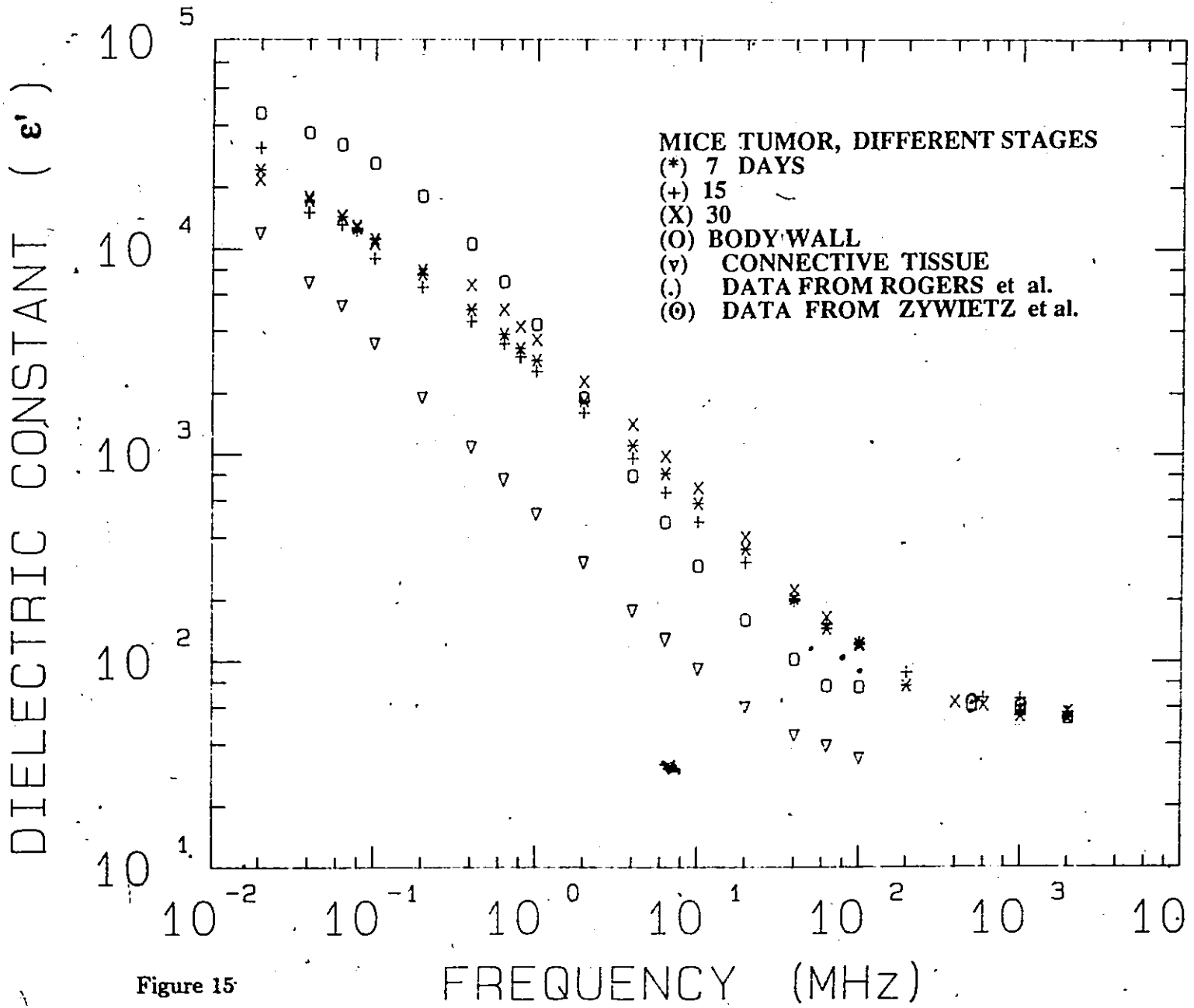

Figure 15

MICE TUMOR (FIBROSARCOMA) DIFFERENT STAGES OF GROWTH

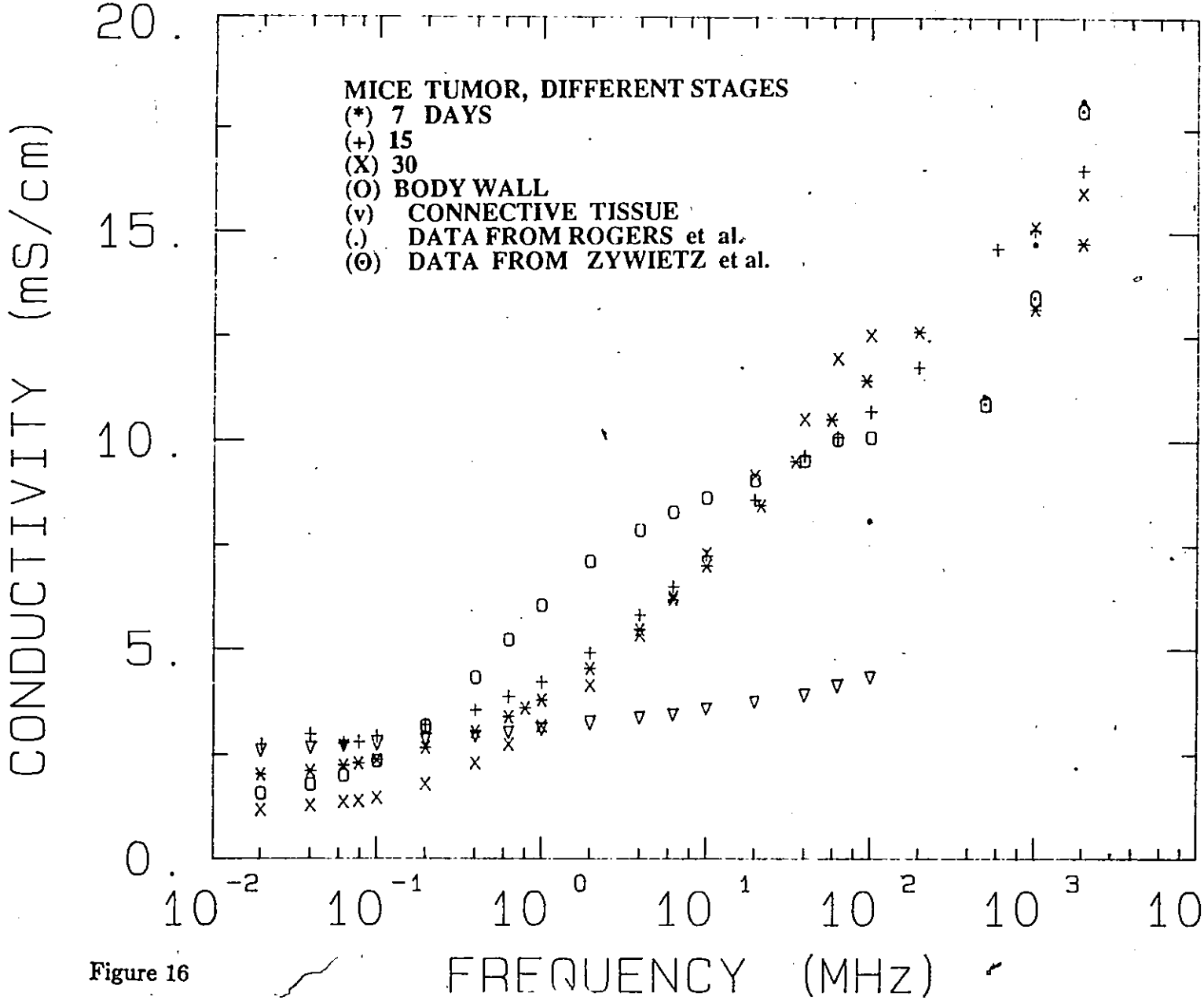

Figure 16

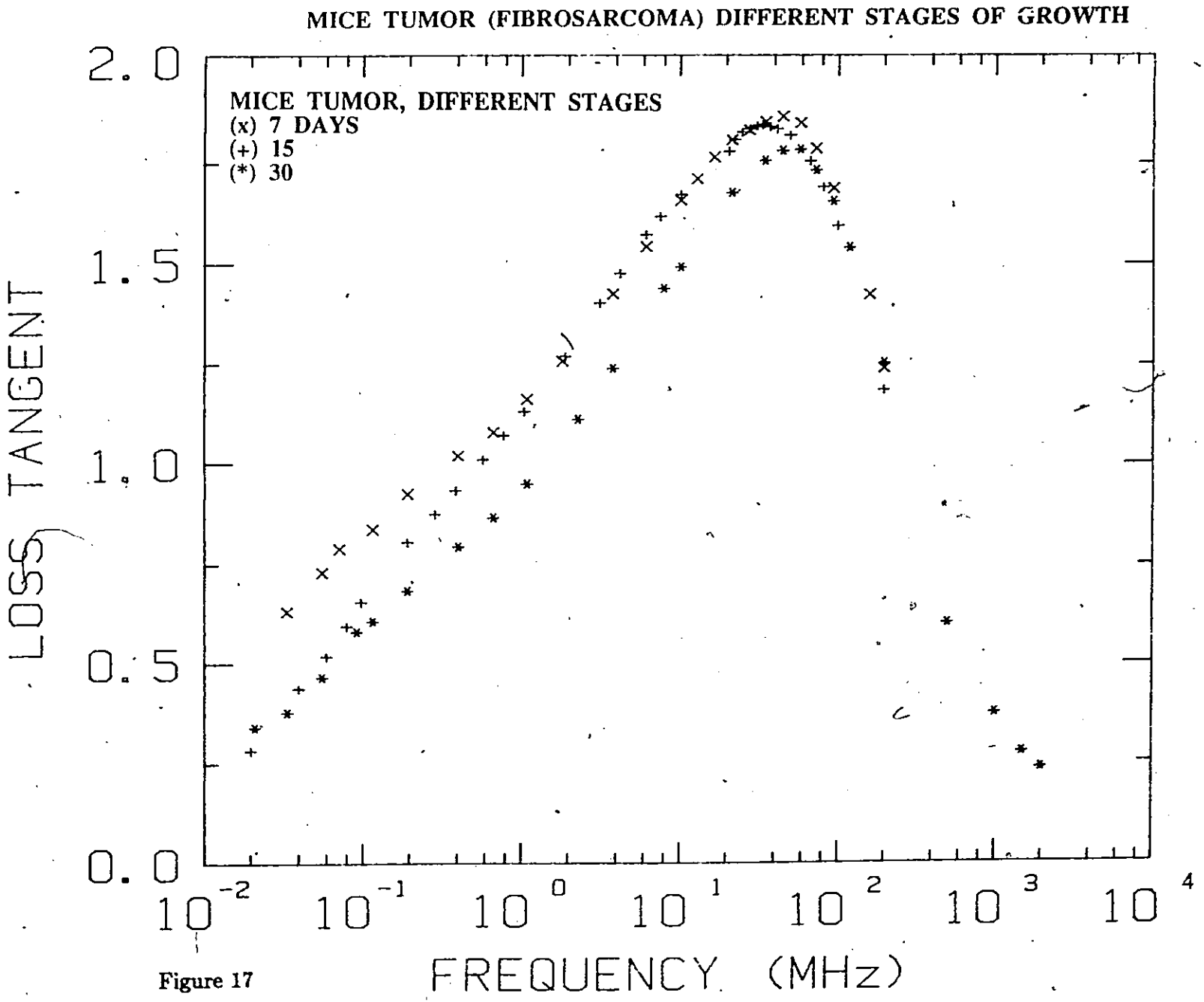
MICE TUMOR (FIBROSARCOMA) DIFFERENT STAGES OF GROWTH
MICE TUMOR, DIFFERENT STAGES
(x) 7 DAYS
(+) 15
(*) 30
LOSS TANGENT
2.0
1.5
1.0
0.5
0.0
10^{-2}
10^{-1}
10^{0}
10^{1}
10^{2}
10^{3}
10^{4}
FREQUENCY (MHz)

Figure 17

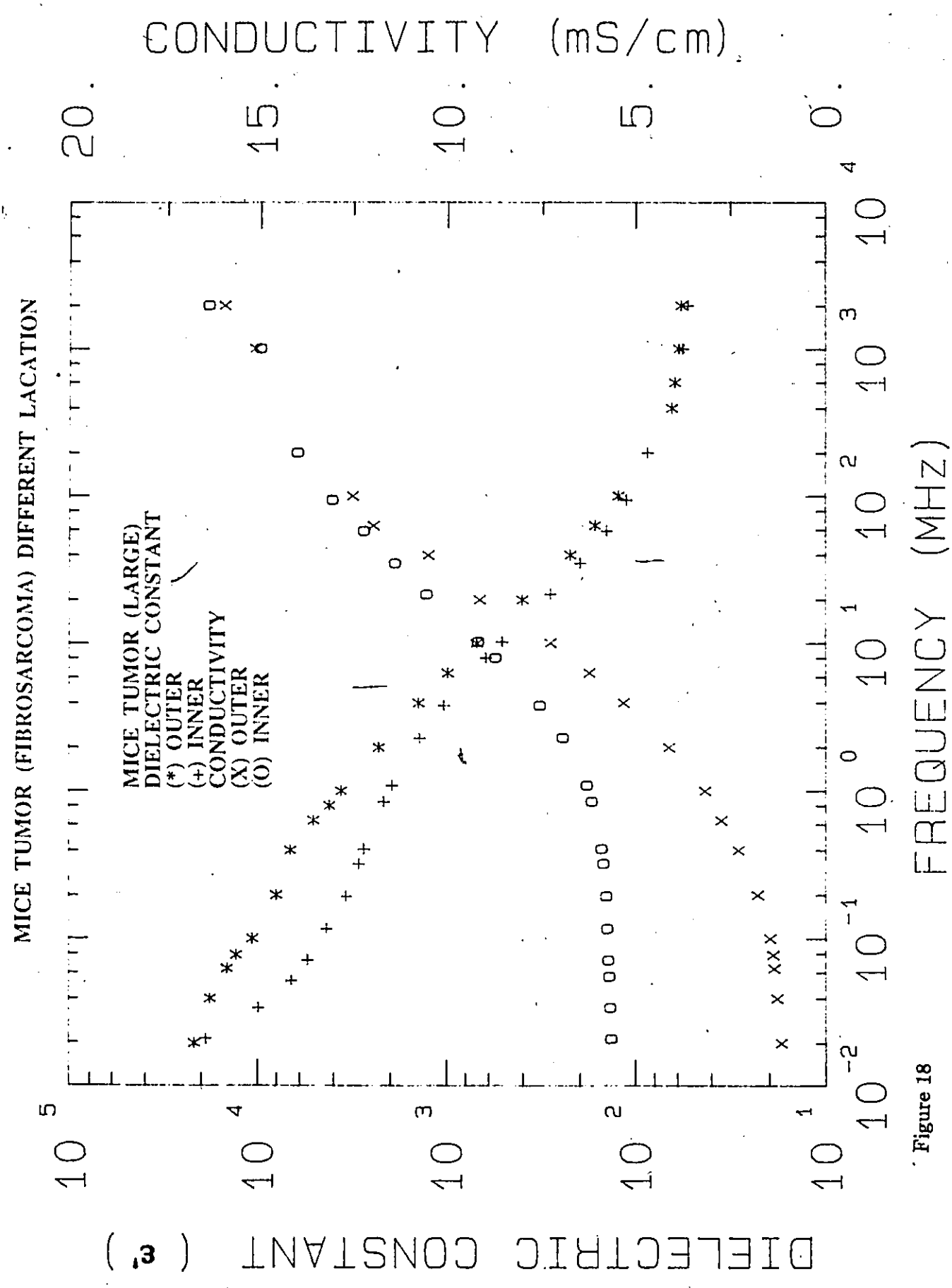
MICE TUMOR (FIBROSARCOMA) DIFFERENT LACATION
MICE TUMOR (LARGE)
DIELECTRIC CONSTANT
(*) OUTER
(+) INNER
CONDUCTIVITY
(X) OUTER
(O) INNER
CONDUCTIVITY (mS/cm)
20.
15.
10.
5.
0.
DIELECTRIC CONSTANT (ε')
10^5
10^4
10^3
10^2
10^1
FREQUENCY (MHZ)
10^-2
10^-1
10^0
10^1
10^2
10^3
10^4

Figure 18

The differences in the dielectric properties of the two regions are quite significant. Figure 19 presents the variation of loss tangent as a function of frequency for the two locations and reveals a shift in the relaxation time of the dispersion.

The water content of each sample was recorded after completion of the measurement procedure (see Table II). All tumor tissues exhibited a high water content compared to that of the normal tissues. However, it was observed that the water content of the outer portion of large tumors showed a decrease by about 1.5 percent whereas that of the necrotic region showed an increase by about 2 percent compared to the average water content of the smaller tumors.

Figures 15 and 16 indicate a dependence of the dielectric constant and the conductivity on the age of the tumor even considering the logrithmic scale employed to plot the data. On comparing the normal tissues with the neoplastic tissues it was observed that the dielectric constant of connective tissue was about three times lower than that of the small tumor at. The dielectric constant of bodywall on the contrary was found to be three times larger than that of the small size tumor at 0.1 MHz but falls rapidly with frequency to a value that is about 2 times lower than that of the small tumor at 10 MHz.

Examining the dielectric properties of the two locations within the large size tumors (outer portion and the inner growing portion), it was found that the dielectric constant of the outer portion was about twice that of the necrotic region while the conductivity of the outer portion was about two to four times lower than that of the necrotic portion. These differences were observed at frequencies below 40 MHz but were small at frequencies above 40 MHz. This observation is consistent with the

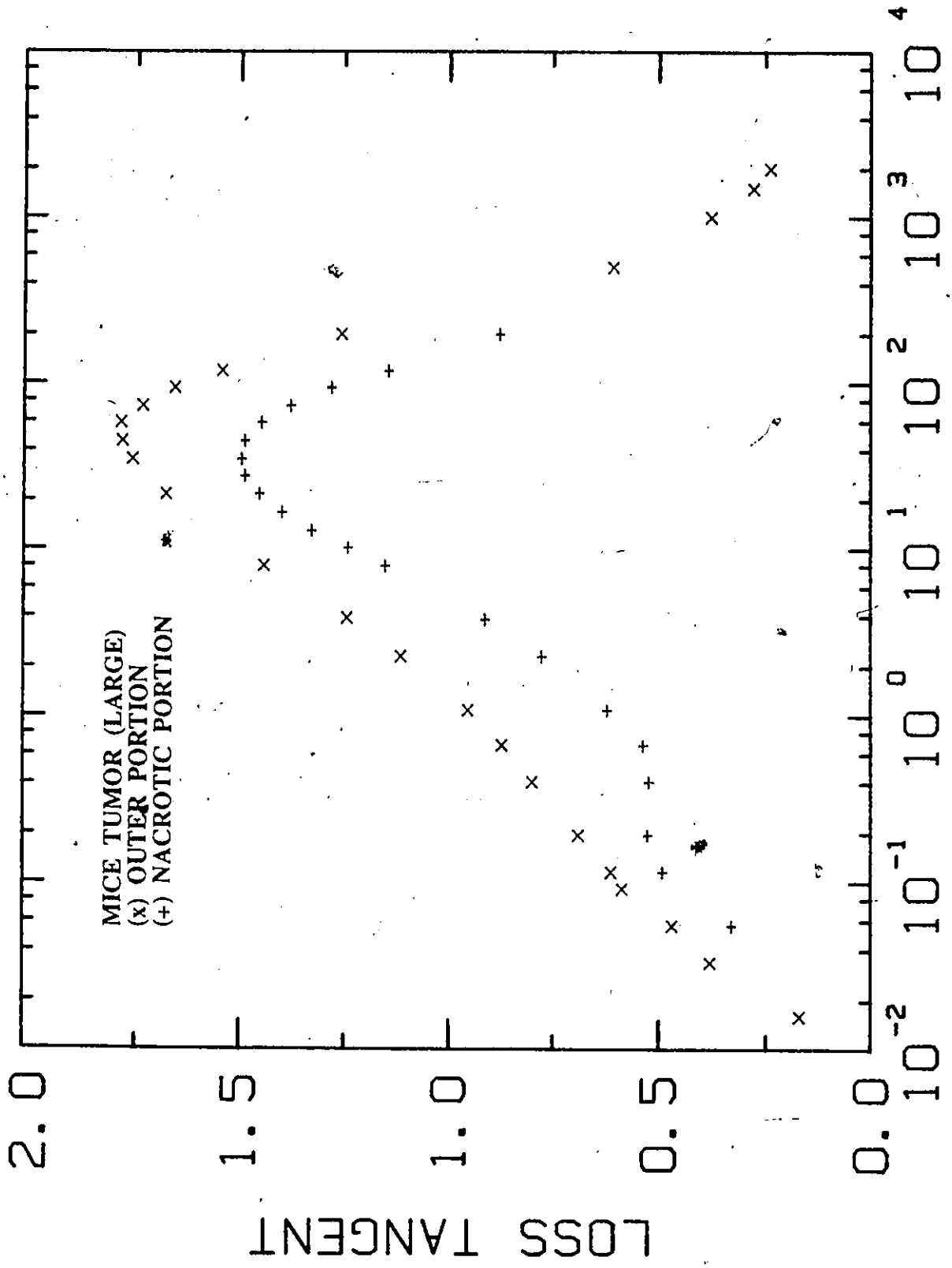
MICE TUMOR (LARGE)
(x) OUTER PORTION
(+) NACROTIC PORTION
LOSS TANGENT
2.0
1.5
1.0
0.5
0.0
10^{-2}
10^{-1}
10^{0}
10^{1}
10^{2}
10^{3}
10^{4}
FREQUENCY (MHz)

Figure 19

TABLE II

Water content of developing tumor tissues

SMALL (OUTER)	MEDIUM (OUTER)	LARGE (OUTER)	LARGE (NACROTIC)
84%	84%	82.5%	86%

conclusion recently drawn by Zywietz and Knochel [1986] from their study of the in vivo dielectric properties of the tumor surface and the necrotic region at frequencies above 200 MHz. Obviously, they did not observe any differences between the two regions at these frequences. It is however, difficult to compare the present data directly with those obtained from previous work. But in order to have a general idea of the magnitude of the dielectric parameters of tumor tissues it would be appropriate to compare the values obtained from previous experiments on fibrosarcomas grown in similar animals (see table III). The data obtained by Rogers et al. [1983] and Zwietz and Knochel [1986] ploted in Figs.15 and 16 are in fairly good agreement with those obtained in the present work. The differences that can be observed may be attributed to a number factors which include (a) different techniques utilized in deriving the tumor, (b) an accuracy of measurement, (c) different environmental conditions, (d) variation in the dielectric properties among animals of the same species and (e) age of samples (time after death).

5.2 Data Analysis And Discussion

Biological systems are typically characterized by four dispersion mechanisms (α, β, γ and δ). Referring to Fig.16 the decrease in the dielectric constant of the tissues between 20 kHz and 400 MHz represents a broad β dispersion. The experimental data that represents this dispersion are usually described in terms of four dielectric parameters; the dielectric constant at the low frequency end of the dispersion (ϵ_s), the dielectric constant at the high frequency end of the dispersion (ϵ_∞), the relaxation time (τ) and the relaxation time distribution (α) which is the measure of the spread of the relaxation time. These parameters for the tumor tissues were obtained using the method based on the dependence of the loss tangent on frequency [Surowiec and

TABLE III

A Summary of the dielectric properties of various tumor tissues grown in animals

SPECIES	FREQ.(MHZ) / SPECIMEN		10.0	100.0	1000.0	10 GHZ	REFERENCE
CANINE (37 C) (IN-VITRO)	HEMANGIO-PERICYTOMA	ε	150	70	55	45	SCHEPPS AND FOSTER [1980]
		σ	11	12	18	102	
	INTESTINAL LCIOMYO-	ε	400	83	60	50	
	SARCOMA	σ	8	10	14	110	
	SPLENIC HAEMATOMA	ε	400	70	47	45	
		σ	6	9	10	105	
MICE (37 C) (IN-VIVO)	LEWIS LUNG CARCINOMA	ε	325	75	60		BURDETTE ET AL [1982]
		σ	5.8	8.8	11		
	MELANOTIC MELANOMA	ε	280	65	46		
	(B16 IMPLANT)	σ	4.6	7.2	12		

SPECIES	FREQ.(MHz) / SPECIMEN		1.0	10.0	100.0	1000.0	10 GHz	REFERENCE
C3H MICE (37 C) (IN-VITRO)	R1F/1 FIBRO-SARCOMA	ε			90	57		ROGERS ET AL [1983]
		σ			8	15		
	KHT FIBRO-SARCOMA	ε			88	59		
		σ			11	17		
RAT MAMMARY CARCINOMA	WALKER 256	ε	3000	-	115	50		PELOSO ET AL [1983]
	MTW9	ε	1200	200	100	50		
	MTW9A	ε	1500	200	75	50		
	9L-GLIOMA	ε	2000	350	120	50		
	MNU	ε	1000	160	-	50		

SPECIES	FREQ (MHz) / SPECIMEN		0.01	0.1	1.0	10.0	100.0	1000.0	REFERENCE
RAT (32.5 C) (IN-VIVO)	R1H RHABDOMYO-SARCOMA	ε						59.9	ZYWIETZ ET AL
		σ						13.3	[1986]
MICE C57/BL (37 C) (IN-VITRO) (30 DAY OUTER PORTION)	MCA1 FIBRO-SARCOMA (PRESENT WORK)	ε	20000	12000	3600	650	120	60	
		σ	1.5	1.9	3.5	7.4	12.4	17.0	

Stuchly;1980] . The loss tangent, obtained as a ratio of the loss factor to the dielectric constant of the material, when plotted as a function of frequency is represented by a bell shaped curve. Fig.17 clearly demonstrates a typical loss tangent curve. The loss factor is given by

$$\epsilon'' = \epsilon_T'' - \frac{\sigma_{DC}}{\omega \epsilon_o} \tag{38}$$

where ϵ_T'' is the total (measured) loss factor, σ_{DC} is the static conductivity and ϵ_o is the dielectric constant of free space. Taking the experimental value of the peak of the bell shaped loss tangent curve ($\tan\delta_m$) and that at $\frac{2}{3}\tan\delta_m$ and the corresponding frequencies f_T and f_1 respectively, the distribution of the relaxation time parameter α can be determmined by numerically solving the following equation (Surowiec and Stuchly;1986):

$$(\frac{f_1}{f_T})^{1-\alpha}[\frac{0.5\ \sin\frac{\alpha\pi}{2}\,(\tan\delta_m + \cos\frac{\alpha\pi}{2}\,\sqrt{\tan^2\delta_m + 1})}{\cos\frac{\alpha\pi}{2} - \tan\delta_m\ \sin\frac{\alpha\pi}{2}} + 3] = (1 + \frac{f_1}{f_T})^{2(1-\alpha)} \tag{39}$$

Once α is known, ϵ_s, ϵ_∞, and τ can be found from the following equations:

$$\sqrt{\frac{\epsilon_s}{\epsilon_\infty}} = \frac{\tan\delta_m + \cos\frac{\alpha\pi}{2}\,\sqrt{\tan^2\delta_m + 1}}{\cos\frac{\alpha\pi}{2} - \tan\delta_m\ \sin\frac{\alpha\pi}{2}} \tag{40}$$

$$\frac{f_T}{f_c} = [\frac{\epsilon_s}{\epsilon_\infty}]^{\frac{1}{2(1-\alpha)}} \tag{41}$$

and

$$\epsilon_c' = \frac{\epsilon_s + \epsilon_\infty}{2} \tag{42}$$

where ϵ_c' is the dielectric constant corresponding to the relaxation frequency f_c which is taken from the experimental data. This method assumes Cole-Cole representation of the dispersion.

The dielectric parameters obtained from the above analysis and using STEPIT program (Stoy et al.1982; Chandler 1975) are presented in tables IV and V, respectively. Several features are evident from these tables. Values of ϵ_∞ and ϵ_s for the two fitting methods are vastly different. Comparing the data for ϵ_s and ϵ_∞ from Figs. 15 and 16 with those in tables IV and V it is clear that the STEPIT program gives more realistic values than the Tanδ method. On the other hand values values of the relaxation frequency f_c and α obtained from the Tanδ seem to be closer to the real values. Note the distinct shift in the frequency of maximum $\tan\delta$ as a function of the age of the tumor (see Fig 17). Refering back to tables IV and V one notes a significant change in the relaxation frequency with the age of the tumor. The relaxation frequency drops from 4.8 MHz to 2.0 MHz and rises to 8.7 MHz. This may refelect both structural and cellular changes during tumor development. It is interesting to note that the relaxation frequency of the necrotic part of the 30-day tumor is only 2.9 MHz. The results presented in tables IV and V clearly indicate the limitations of both parameter fitting techniques; eg. STEPIT and the Tanδ method. Extreme care and caution is required in the fitting procedures and interpratation of the results.

Table IV **MICE TUMOR (FIBROSARCOMA)**

DIELECTRIC PARAMETERS

TIME(DAYS)	7	15	30	30
LOCATION	OUTER	OUTER	OUTER	INNER
PARAMETERS				
ε_s	1940	3180	1378	2560
ε_∞	40	35	46	50
f_c(MHz)	4.8	2.0	8.7	2.9
α	0.3	0.2	0.1	0.2
σ_{DC} (mS/cm)	2.0	2.1	0.8	5.5

TABLE V

DIELECTRIC PARAMETERS USING STEPIT PROGRAM

TIME	7	15	30	30
LOCATION	OUTER	OUTER	OUTER	INNER
PARAMETERS				
ε_s	16133	11690	11484	4298
ε_∞	10	39	10	15
f_c(MHz)	0.18	0.26	0.48	0.93
α	0.32	0.3	0.29	0.32
σ_{DC} (mS/cm)	2.1	2.9	1.4	5.6

As discussed in chapter II there are several dielectric relaxation mechanisms, each of which predominate in tissues at various frequency ranges. These include dipolar reorientation of tissue water molecules (microwave frequencies), charging of cell membranes and dipolar reorientation of protien dipoles (radio frequencies), ionic diffusion along membrane surfaces (audio frequencies), and other smaller effects at various frequency ranges depending on the complexities of the tissue structure. In tissue, evidently several mechanisms overlap with a broad distribution in effective relaxation times. The relative permittivity continually decreases with no plateaus indicating no clear transition from one mechanism to another. A similar distribution is seen in Fig.15. where the dielectric dispersion curve represents a broad β dispersion as well as the tail end of the α dispersion at lower frequencies. The processes that are primarily responsible for the β - dispersion are the charging of the cell membranes and the dielectric relaxation of the protien molecules. Although an exact mathematical representation of the dielectric behaviour of the tumor in terms of its structure is not possible, a good approximation is to assume that the tissue is composed of cellular and sub - cellular components of different types. The theory is based on Maxwell - Wagner mixture theory [Schwan, 1957; Stoy et al.,1982]. According to this theory, for a suspension of membrane covered non - conducting spheres of volume fraction p, having radius R, internal condictivity σ_i and specific capacitance C_m, suspended in an electrolyte of conductivity σ_a the suspension will show a dielectric relaxation described by the following equations.

$$\epsilon_s - \epsilon_\infty = \frac{9}{4\epsilon_o} pRC_m \qquad (43)$$

$$f_c = \frac{\sigma_a}{3\pi R C_m} \tag{44}$$

$$\sigma_{DC} = \sigma_a(1 - 3\frac{p}{2}) \tag{45}$$

The typical diameter of the mice Fibrosarcoma cells were between 20 to 25 μm (Dr. S.Kadhim, Cancer Clinic, Civic Hospital, Ottawa). Assuming the specific membrane capacitance to be 10^{-2} F/m^2 (Foster and Schepps, 1982),the contribution of the outer cell membrane to the bulk permittivity at low frequencies was calc ed using the above equations. For small and medium size tumors the calculated permittivity increase was about 5.10^3. The corresponding values for the outer portion and the necrotic region of the large tumor was about 5600 and 4500 respectively with a relaxation frequency at about 5 MHz. It is noted that the volume fraction of the small and the medium size tumors is the same resulting in identical permittivity increase. However the volume fraction of cells in the necrotic region was much smaller due to higher water content showed a smaller permittivity increase. The observed permittivity values below 1MHz is considerably higher reflecting the contributions from other polarization effects. The dielectric relaxation arising (see Fig.15) from the charging of the cell membranes is spread over a wide frequency range (almost four decades in frequency above 100 kHz) with contributions from the cell membranes dominating at frequencies below 1 MHz, while the polarization effects from protein molecules, intracellular membraneous structure contributing at frequencies up to 100 MHz (Foster and Schepps, 1981). At frequencies above 100 MHz the changes in the permittivity and conductivity with fre-

quency probably reflects relaxation of protein - bound water as well as other sources which are not presently well understood.

The conductivity of 7-day tumors, as seen in Fig.16 is approximately twice than that of 30 day tumors at 20 kHz. These differences decrease with frequency up to about 8 MHz, but start increasing again in the reverse manner, at frequencies above 10 MHz. This is in agreement with the conclusions by Purdome et al [1958] on MC1M mouse sarcoma line which indicated an increase in the negative electrical charge on cellular surface as the cells transform from normal to tumor cells. They further suggested that as the transformed cells acquire more malignant properties there is a further increase in negative charge. Hence, an increase in mobile electrical charges on the surface of the cellular membranes would also increase the electrical conductivity of the tissue as these charges would be displaced and by the microwave field.

The variation of the conductivity with frequency at frequencies below 1 MHz is slow and is dominated by the ionic conductivity of the specimen. At these frequencies the cell membrane presents a high impedance to the current resulting in a nearly complete exclusion of the intra-cellular conductivity. This reflects the presence of higher proportion of biological macromolecules and hence less water content (see Table II). These molecules not only reduce the volume available for ion conduction but also have high ionic binding properties. The rapid increase in the conductivity at frequencies above 1 MHz reflects the net water and electrolyte content of the tumor, since the impedance presented by the cell membranes at these frequencies is very low. The total conductivity of the specimen in this frequency region is the weighted average of the conductivities of the intra-cellular and extra-cellular regions. High ionic conductivity of the medium tumor could be attributed to fact that the sample might have been contained some necrotic tissues as the necrotic region was not well defined.

The necrotic region of a malignant tumor is a nutrient depleted region consisting mainly of dead cell fragments, high concentration of ions and high water content. As can be seen from Fig.18 the conductivity of the necrotic portion is about two to four times higher than that of the outer portion which is well oxygenated. To our knowledge there has been only one report on the study of the dielectric properties of different regions within the tumor. Zywietz and Knochel [1986] have reported the dielectric properties of mice tumor (rhabdomyosarcoma) at different depths within the tumor (specifically the tumor surface and the necrotic center) at frequencies between 200 MHz and 2.4 GHz. No variations in these properties were however observed in that frequency range. This supports the present findings as at frequencies above approximately 100 MHz the differences between the two regions are barely visible.

The observed dielectric properties of the three stages of mice fibrosarcoma as a function of tumor development reflect the structural changes at the cellular level within the tumor. Cell transformation is accompanied by many changes in the membrane ultrastructure. In general, changes in the proportion of lipids, cholesterol content, insertion of abnormal protein molecules and increase in cell size are all mechanisms possibly responsible for perturbing the membrane structure. Another important factor to be considered is the tissue water content. The neoplastic tissues have higher water content than the normal tissues. It has been shown [Foster and Schepps 1980] that the dielectric properties of soft tissues are dependent on their water content. Therefore, the observed behaviour of the three tumor stages could be attributed, in part, to changes in the structure of water during cell transformation. This is consistent with the theory proposed by Ling [1962] who states that the interaction between water and cellular macromolecules causes exclusion of certain solutes in the cytoplasm resulting in asymmetric distribution of sodium and potassium ions. This theory predicts changes

in the physical properties of tissue water during cell transformation as (a) electrolyte concentration change, (b) groups of macromolecules undergo conformational changes and (c) cell composition alters. In view of the above theory numerous nuclear magnetic resonance (NMR) experiments have been performed, and the results have been applied to the study of biological water in cancer. With this technique the characteristic of hydrogen nuclei of tissue water could be examined in a non-destructive manner in living cells. These experiments have also shown that the relaxation times of water protons in rat fibrosarcoma were significantly higher than the corresponding normal tissues. It was also reported by Frey et al. [1974] that some uninvolved organs in an animal bearing a tumor could demonstrate elevated spin lattice relaxation times (T1) for water protons when compared to the same organ in animals without tumors.

Since the differences in the dielectric properties of different tumor stages are significant although not very large they might be exploited for tumor detection and characterization of malignant tumors. The pronounced difference in the bulk electrical properties of tumor and surrounding normal tissues could be exploited in optimization of the energy absorption pattern when using electromagnetically induced hyperthermia for tumor heating.

CHAPTER VI

Conclusions

The study of the dielectric properties of fibrosarcoma (MC1A) induced in mice was performed in a broad frequency range covering radiowave and microwave frequencies using frequency domain measurement techniques. Two computer - controled automatic network analyzers were used enabling the measurements to cover a frequency range from 10 kHz to 2 GHz. The dielectric constant and the conductivity of the sample were obtained from the input reflection coefficient of specially designed coaxial transmission line sensors . Tumor tissues at three different stages of development were measured. For comparison normal surrounding tissues such as connective and body wall (muscle) were also investigated. The main objective of the present investigation was to characterise the development of tumors in terms of their dielectric properties (dielectric constant and conductivity) that could contribute to the various aplications of EM energy cited in the first chapter.

From the analysis of the data it has been observed that the dielectric constant of the growing fibrosarcoma exhibits variations with age. The conductivity of these tissues similarly show a dependence on age. This variation as a function of tumor development emphasizes a possible use dielectric spectroscopic techniques for imaging and characterisation of tumors and their early detection. In order to obtain better resolution of various factors contributing to the relaxation process other methods of analysis e.g. Cole-Cole plots, complex conductivity plots are neede to be studied.

The present investigation also indicates a drop in the dielectric constant value, increase in the conductivity value and an increase in the water content of the nacrotic

portion of the large tumor. This would suggest an increase in the ionic concentration of the medium and collapsing of the cellular structures. Although the system is highly complex, the evidence of the elevated permittivity and a shift of the relaxation frequency of the developing tissue certainly indicates that changes in the cellular membranous structures including increase in the cell size, an insertion of abnormal protein molecules, an increase in water content, changes in the physical properties of water may be the dominating features during cell transformation. For diagnostic and therapeutic (hyperthermia) applications such differences might be of greater practical significance.

Further work is needed in the study of developing tumor tissues as well as to determine the extent of heterogeneity of a tumor specimen. The data would be extremely useful in developing microwave applicators for treating tumors and microwave and radiowave imaging systems for detection of tumors. An important aspect is to study, whether the dielectric properties of induced tumors could be used to predict the dielectric properties of spontaneous tumors of a similar nature. As observed in the present study at low frequencies, the conductivity of tumor tissue is strongly influenced by necrosis because of inadequate nutrient supply in their interiors. In culture tumor nodules develop necrosis at a very early stage. For the same reason tumors induced in animals can be presumed to exhibit necrosis whose extent will depend on the details of microcirculation. Follow-up study of spontaneously occuring tumors would be useful for comparison. Moreover, a more extensive comparison between benign and neoplastic tissues is needed.

References

Ackmann,J.J. and Seitz,M.A. "Methods of Complex Impedance Measurements in Biologic Tissues" CRC Critical Review in Biomedical Engineering, vol. 11, pp 281-311, 1984.

Athey,T.W., Stuchly,M.A. and Stuchly.S.S. "Measurement of Radiofrequency Permittivity of Biological Tissues With an Open-Ended Coaxial Line: Part I" IEEE Trans. M.T.T. vol 30, pp82-86, 1982.

Berberian J.G. and Cole,R.H. "Low Frequency Bridge for Gaurded Three Terminal and Four-Terminal Measurement of Admittance", Rev.Sci.Instrum., vol 40, pp.811-817, 1969.

Boned,C. and Payrelasse,J. "Automatic Measurement of Complex Permittivity (from 2 MHz to 8GHz) Using Time Domain Spectroscopy", J. Phys. E: Sci. Instrum., vol 15, pp 535-538, 1982.

Bottcher,C.J.F. "Theory of Electric Polarization" vol.1 (Elsevier publication, Amsterdam)

Bottreau,A.M., Dutuit,Y. and Moreau,J. J.Chem,Phys., vol.66, pp 333, 1977

Burdette,E.C., Seals,J. Toller,J.C., Cain,F.L. and Magin,R.L. "Preliminary in-vivo Probe Measurements of Electrical Properties of Tumors in Mice" in Digest IEEE MTT-S, Microwave Symposium San Diego, CA, 1977.

Bussey, H.E. "Measurement of RF Properties of Materials - A Survey", Proc. IEEE, vol. 55, pp 1046 - 1053, 1967.

Chandler,J.P. Quantum Chemistry Program Exchange, Indiana University, 1975

Chaudhary,S.S., Mishra,R.K.,Swarup,A. and Thomas,J.M. "Dielectric Properties of Normal and Malignant Human Breast Tissues at Radiowave and Microwave Frequencies." Ind. J. biochem. and Biophys, vol.21, pp 76-79, 1984.

Cheung,A.Y., "Microwave and radiofrequency techniques for clinical hyperthermia", Br. J. Cancer, vol. 45,Suppl.V, 16, pp 16-24, 1981.

Cole,R.H. "Time Domain Reflectrometry" Ann. Rev. Phys. Chem., vol.28, 283-300, 1977

Cole,K.S. and Cole,R.H. "Dispersion and Absorption in Dielectrics I. Alternating Current Characteristics", J. Chem Phys. vol. 9, pp 341-351, 1941.

Cole,R.H. and Gross, P.M. "A Wide Range Capacitance-Conductance Bridge ", Rev. Sci. Instrum. vol.20, pp 252-260, 1949.

Cole,K.S. and Kishimoto,U. "Platinized Silver Chloride Electrode", Science, vol. 136, pp 381-382, 1962.

Cook,H.F. "The Dielectric Behaviour of Some Types of Human Tissues at Microwave Frequencies", Br. J. Appl. Phys. vol.2, pp 295-300,1951.

Damadian,R. "Tumor Detection by Nuclear Magnetic Resonance", Science, vol 171, pp 1151-1153, 1971.

Davidson, D.W. and Cole,R.H. "Dielectric Relaxation in Glycerine", J. Chem. Phys. vol.18, pp 1417, 1950.

Dukhin,S.S. "Dielectric Properties of Disperse Systems", in Surface and Colloidal Science vol.3, pp 83 - 165, 1971.

England and Sharples "Dielectric Properties of Human Body in The Microwave Region of the Spectrum",Nature, vol 163, pp 487, 1949

Fatt,G., and Fatt,P. "Linear Electrical Properties of Striated Muscle Fibers Observed with Intracellular Electrodes", Proc. Roy.Soc.London, B, vol. 160, pp64,1964

Ferris, C.D. Introduction to Bioelectrodes, Plenum Press, New York, 1974.

Ferry,J.D. and Oncley,J.L. J.Amm Chem.Soc., vol.63, 272, 1941.

Foster,K.R. and Schepps,J.L. "Dielectric Properties of Tumor and Normal Tissues at Radio through Microwave Frequencies" J.Microwave Power, vol. 16, pp 107-119, 1981.

Foster K.R. and Schwan, H.P. "Dilectric Properties of Tissues - A review, 1985

Frey,H.W., Knispel,R.R., Kruvv,J., Sharp,A.R., Thompson,R.T. and and Pintar,M.M. "Proton Spin-Lattice Relaxation Studies of Non-Malignant Tissues of Tumorous Mice", Natl. Cancer Inst., vol 49, pp 903-906, 1972.

Fricke,H. "The Theory of Electrolyte Polarization", Phil. Mag. vol.14, pp 310-318, 1932.

Fricke,S. and Morse,S. "The,Electric Capacity of Tumors of The Breast", J. Cancer Res. vol.16, pp 310-376, 1926.

Friedenthal,E., Mendecki,J., Botstien,C., Sterzer,F., Nowogrodzki,M. and Paglione,R. "Some practical consideration for the use of localized hyperthermia in the treatment of cancer", J. Microwave Power, vol.16, pp 199-204, 1981.

Geddes,L.A., Da Costa,C.P. and Wise,G. "The Impedance of Stainless Steel Electrodes", Med.Biol.Eng. vol. 9, pp 511-521, 1971.

Grant,E.H. Br. J. Appl. Phys. vol.6, pp 181, 1955.

Grant,E.H., Sheppard,R.J. and South,G.P. "Dielectric Behaviour of Biological Molecules in Solutions", Clarendon Pres, Oxford, 1978.

Hand,J.W. "Physical techniques for delivering microwave energy to tissues," Br. J. Cancer, vol. 45, Suppl.V, 9-15,1982.

Hartshorn,L. and Ward,W.H. J. Inst. Elect. Engrs. (london), vol. 79, pp 597, 1936.

Havriliak,S. and Negami,J. "A Complex Plane Analysis of Alph Dispersion in Some Polymer Systems", J. Polym. Sci.,C., vol. 14, pp 99, 1966.

Hayakawa,R., Kanada,H., Sakamoto,M. and Wada,Y. "New Apparatus for Measuring the Complex Dielectric Constant of Highly Conductive Materials", Jap. J. Appl. Phys., vol. 14, pp 2039-2052, 1975.

Hazelwood,C.F., Cleveland,G. and Medina,D. "Relationship Between Hydration and Proton Nuclear Magnetic Resonance Relaxation Times in Tissues of Tumor Bearing and Non-Tumor Bearing Mice : Implications for Cancer Detection", Natl. Cancer Inst. vol.52, pp 1849-1853, 1974.

Hill,N.E., Vaughan,W.E., Price,A.H. and Davies,M. in Dielectric Properties and Molecular Behaviour , Van Nastrand Reinhold Company, 1969.

Iskander,M.F. and Stuchly,S.S. "A Time Domain Technique for Measurement of The Dielectric Properties of Biological Substances", IEEE Trans. Instrum. Meas., vol.21, pp 425-429, 1972.

Joines,W.T., Jirtle,R.L., Rafal,M.D. and Schaefer,J. "Microwave Power Absorption Differences Between Normal and Malignant Tissues", Int. J. Radiation Oncology Biol.Phys., vol.6, pp 681-687, 1980.

Jones,G. and Bollinger,G.M. J.Amm.Chem.Soc., vol 57, pp 280, 1935.

Kaatze,V. and Gieze,K. Dielectric Relaxation Spectroscopy of Liquids : Fre-

quency Domain and Time Domain Experimantal Methods", J.Phys.E.: Sci. Instrum., vol.13, pp 133-141, 1980.

Kraszewski,A., Stuchly,M.A., Stuchly,S.S. and Smith,A.M. "In-Vivo and In-Vitro Dielectric Properties of Animal Tissues at Radio Frequencies", Bioelectromagnetics, vol.3, pp 421-432, 1982.

Kraszewski,A., Stuchly,S.S., Stuchly,M.A. and Symons,S.A. "On The Measurement Accuracy of the Tissue Permittivity In Vivo", IEEE Trans. Instrum. Meas., vol.32, pp 37-42, 1983.

Ling,G.N. "The Physical Theory of the Living State", Blaisdell, Philadelphia, Pennsylvania, 1962.

Mendecki,J., Friendenthal,E., Botstien,C., Sterzer,F., Pagoline,R., Nowogrodzki,M. and Beck,E. "Microwave induced hyperthermia in cancer treatment, apparatus and preliminary results," Int.J. Radiation Oncology biol.phys., vol. 4, pp 1095-1103, 1978.

Mishra,R.K., Chaudhary,S.S. and Swarup,A. "Recent Advances in Time Domain Spectroscopy", J.Scientific and Indust. Res., vol 42, pp 548-556, 1983.

Oliver,B.M. H.P.Application Note, No 62 (Hewlett-Packard Co. Palo Alto, CA), 1964.

Peloso,R., Tuma,D.T. and Jain,R. "Dielectric Properties of Solid Tumors During

Normothermia and Hyperthermia", IEEE Trans. Biomed. Eng. vol.31, pp 725-728, 1984.

Purdome,L. and Ambrose,E.J. "A Correlation Between Electrical Surface Charge and Some Biological Characteristics During Stepwise Progression of a Mouse Sarcoma", Nature, vol. 181, pp 1586-1587, 1958.

Redheffer,R.M., "The Measurement of Dielectric Constant", in Techniques of Microwave Measurements, C.G.Montgomery, Ed. New York: McGraw Hill, 1947, Ch.10, pp 561-676.

Roberts,S. and von Hippel,A. Br.J.Appl.Phys. vol. 6, pp 181, 1955.

Rogers,J.A., Sheppard,R.J., Grant,E.H., Bleehen,N.M. and Honess,D.J. "The Dielectric Properties of Normal and Tumor mouse Tissue between 50 MHz to 10 GHz., Br. J. Radiology, vol.56, pp 335-338, 1983.

Rzepecka,M.A. and Stuchly, S.S. "A Lumped Capacitance Method for the Measurement of the Permittivity and Conductivity in the Frequency and Time Domain- A Further Analysis", IEEE Trans. Instrum. Meas., vol.24, pp 27-32, 1975.

Schepps,J.L. and Foster,K.R. "The VHF and Microwave Dielectric Properties of Normal and Tumor Tissues - Variation in Dielectric Properties with Tissue Water Content", Phys.Med.Biol, vol.25, pp 1149-1159, 1980.

Schwan,H.P. "Interaction of microwave and radiofrequency radiation with biological systems", IEEE Trans.on MTT, vol MTT-19, pp 146-152, 1971

Schwan, H.P. "Electrical Properties of Tissues and Cell Suspensions", in Advances in Biological and Medical Physics, vol.5, Academic Press, New york, pp 147-209, 1957.

Schwan,H.P. "Electrical Properties of Cells: Principles, some Recent Results and Some Unresolved Problems", in the Biophysical Approach to Excitable Systems, W.S.Adelman and D.Goldman, eds., Plenum Press, New York, pp 3-24, 1981.

Schwan,H.P. and Sittel,K. "Wheatstone Bridge for Admittance Determination of Highly Conducting Materials at Low Frequencies", Amm. Inst. Elect. Engrs. Trans. AIEE, vol. 72, pp 114, 1953.

Schwan,H.P. "Determination of Biological Impedances", in Physical Techniques in Biological Research, ed: William Nastuk, Vol VI Acad Press, 1963.

Schwan,H.P. and Maczuk,J. "Simple Technique to Control the Stray Field of Electrolytic Cells", Rev. Sci. Instrum., vol. 31, pp 59-62, 1960.

Schwan,H.P. and Maczuk,J.G. "Electrode Polarization Impedance; Limits of Linearity", Proc. 18th Ann.Conf. Eng. Biol. Med., Philadelphia, Pa, ed: Mcgregor and Warner, pp 270, 1965.

Schwan,H.P. and Ferris,C.D. "Four-Electrode Null Techniques for Impedance

Measuremen with High Resolution", Rev. Sci. Instrum., vol. 39, pp 481-485, 1968.

Shaw, T.M. "The Elimination of Errors Due to Electrode Polarization in Measurements of Dielectric Constants of Electrolytes", J. Chem. Phys., vol. 10, pp 609-617, 1942.

Singh,B., Smith,C.W. and Hughes.R. "In-Vivo Dielectric Spectrometer", Med. and Biol. Eng. and Comput., vol. 17, pp 45-60, 1979.

Simpson,R.W., Berberian,J.G. and Schwan,H.P., "Non-Linear AC and DC Polarization of Platinum Electrodes", IEEE Trans. Biomed.Eng., Vol. 27, pp 166-171, 1980.

Sterzer,F. "Localized hyperthermia treatment of cancer", RCA Review, vol. 42, pp 727-751, 1981.

Stoy,R.D., Foster K.R. and Schwan.H.P. "Dielectric properties of mammalian tissues from 0.1 to 100 MHz : A summary of recent data", Phys. Med. Biol. vol. 27, pp 501-513, 1982.

Stuchly,M.A. "Interaction of Radiofrequency and microwave radiation with living systems" Radiation and Environm.Biophys. vol. 16, pp 1-14, 1979

Stuchly, M.A. and Stuchly S.S. "Dilectric properties of biological systems - Tabulated", J. Microwave Power, vol.15, 19-26, 1980.

Stuchly,M.A., Brady, M.M., Stuchly,S.S. and Gajda,G. "Equivalent Circuit of an Open Ended Coaxial Line in a Lossy Dielectric" IEEE Trans Instrum. Meas., vol. 31, pp 116-119, 1982.

Stuchly,M.A., Athey,T.W., Samaras,G.M. and Taylor,G.E. "Measurement of Radiofrequency Permittivity of Biological Tissue with an Open Ended Coaxial Line. Part II Experimental Results. IEEE Trans M.T.T., vol. 30, pp 87-92, 1982.

Stuchly,S.S., Rzepecka,M.A. and Iskander,M.F. "Permittivity Measurements at Microwave Frequencies Using Lumped Elements", IEEE Trans. Instrum. Meas., vol. 23, pp 56-62, 1974.

Stuchly,M.A. and Stuchly,S.S. "Coaxial Line Reflection Methods for Measuring Dielectric Properties of Biological Substances at Radio and Microwave Frequencies,- A Review", IEEE Trans. Instrum. Meas., vol. 29, pp 176-183, 1980.

Studwell,M.L., Burdette,E.C. and Freeman,D.J. "Non-Invasive Measurement of Dielectric Properties, Differences in Solid Tumor and Normal Host Tissue", Radiation Research, vol. 94, pp 594-595, 1983.

Surowiec,A., Stuchly,S.S. and Swarup,A. "Radiofrequency Dielectric Properties of Animal Tissues as a Function of Time Following Death", Phys. Med. Biol., vol.30, pp 1131-1141, 1985.

Surowiec,A. Stuchly,S.S. and Swarup,A. "Postmortem Changes of the Dielectric

Properties of Bovine Brain Tissues at-Low Radiofrequencies", Bioelectromagnetics, vol.7, pp 31-43, 1986.

Takashima,S. "Effect of Ions on The Dielectric Relaxation of DNA", Biopolymers, vol. 5, pp 899-913, 1967.

Takashima,S. J.Polymer Science, Part A, vol 1, pp 2791, 1963.

Tinga, W.R. and Nelson. S.O., "Dilectric properties of materials for microwave processing - Tabulated" J. Microwave Power, vol. 8, pp 23-65, 1973.

Voss,G. and Happ,H. "Time Domain Spectroscopy (TDS) of Dielectric Properties up to 15 GHz with Voltage Pulses. Application to Solids and Liquids", J. Phys.E: Sci. Instrum., vol. 17,pp 1984.

van Gemert, M.J.C. "High Frequency Time Domain Methods in Dielectric Spectroscopy", Phillips Res. Rept., vol.28, pp 530-572, 1973.

van der Touw,F. and Mandel,M. "Plane-Parallel Condenser with Variable Electrode Spacing for Determination of Electrical Permittivity of Highly Conducting Liquids Below 1 MHz. Pt.I Theoretical Consideration", Trans. Faraday Soc., vol. 67, pp 1336-1360, 1971.

Voss,G. and Happ,H. "Time Domain Spectroscopy (TDS) of Dielectric Properties up to 15 GHz with Voltage Pulses. Application to Solids and Liquids", J. Phys.E: Sci. Instrum., vol. 17,pp 1984.

Westphal,W.B. "Distributed Circuits" in Dielectric Materials and Applications; ed. A. von Hippel, 1954.

Zywietz,F. and Knoechel,R. "Dielectric Properties of Co- Y - Irradiated and Microwave Heated rat Tumor and Skin Measured in-Vivo Between 0.2 to 2.4 GHz", Phys. Med. Biol., vol. 31, pp 1021-1029, 1986.